

1
2
3
4
5
6
7
8
9
10
11
12
13
14
15

On the modification of tides in
shallow water regions by wind effects

by

J. Eric Jones and Alan M. Davies
Proudman Oceanographic Laboratory
6 Brownlow Street
Liverpool
Merseyside L3 5DA
U.K.

1 ABSTRACT

2 The influence of non-linear effects upon tides in shallow coastal regions, due to the
3 presence of a significant storm surge is examined using a two-dimensional model of the west
4 coast of Britain. The model has an unstructured grid, designed to have a high resolution mesh
5 in the near coastal region of the eastern Irish Sea, the area chosen as the focus of this study.
6 The influence of tide-surge interaction upon the M_2 , M_4 and M_6 components of the tide, due
7 to surges produced by steady uniform wind stresses is examined in detail. Calculations show
8 that in deep regions the tide is unaffected by the surge. However, in shallow coastal regions
9 there is significant modification of tidal elevations and currents. This arises because of
10 changes in bottom stress, and the non-linear interaction term in the hydrodynamic equations.
11 In addition the locations of regions that “wet and dry” are changed during the tidal cycle due
12 to the influence of the surge. This gives rise to significant spatial variations and changes in
13 magnitude of the tide and its higher harmonics depending upon wind stress direction and
14 water depth. These results explain why tidal energy remains in the surge residual in shallow
15 water when it is computed by de-tiding the total signal using a tide only calculation; an effect
16 often found in observed surge residuals.

17

1. INTRODUCTION

The effect of tide-surge interaction due to non-linear processes in shallow water regions upon surge elevations has been known for some time (e.g. Prandle and Wolf (1978), Horsburgh and Wilson (2007), Bobanovic et. al. (2005), Bernier and Thompson (2006) and review of Heaps (1983)). However, the conventional approach of predicting total elevations due to tides and surges has been to linearly decompose the total into its tidal and surge components. By this means the tidal elevation contribution to the total was determined from the harmonic analysis of long term (of order a year or more) observed elevations. These were then used to accurately predict tidal elevations at ports. The surge component was computed using a hydrodynamic model. Initially these models used a coarse finite difference grid and did not take account of tidal effects (e.g. Heaps, 1965, 1969). Since tide surge interaction is negligible in deeper water, and the grid of these models was so coarse that they could not resolve nearshore regions then the neglect of tides was appropriate. However, as grids were refined, and shallow regions resolved then it became necessary to take account of tides in order to get the appropriate level of friction and interaction in the model. In order to separate the surge from such a calculation, the model was run with tidal forcing only and this solution subtracted from the tide and surge to give the surge component. The prediction of total water level that was required for flood defence purposes was then derived by adding this surge to the tide derived from harmonic analysis. In essence a linear decomposition was assumed, although in shallow water such a decomposition was strictly not possible due to non-linear effects.

The difficulty of de-tiding a tide and surge calculation in shallow water by subtracting a tidal solution was clearly shown by Jones and Davies (2007a). They found using a number of orthogonal wind components that the steady state surge elevation was significantly affected by detiding the solution at high or low tide. This arose because the level of

1 interaction between tide and surge depended upon the state of the tide, and how the surge had
2 modified the tide. Consequently de-tiding a tide and surge calculation by subtracting a tide
3 only solution, left energy at the tidal period within the surge. In addition observed surge
4 records in shallow water regions derived by subtracting a tidal time series (based upon the
5 harmonic analysis of a year long record) were found to contain energy at tidal frequencies.
6 This suggests that besides tide-surge interaction influencing the surge it also modifies the tide
7 at the time of the surge in shallow water regions.

8 As the effect of tide-surge interaction upon the surge has been extensively studied
9 (e.g. Prandle and Wolf (1978)), as have the non-linear processes that produce this interaction
10 and hence modify the surge, namely the non-linear momentum advection terms, and
11 quadratic bottom friction, it is not our intention here to focus on the surge. Rather our aim is
12 to focus on how tidal harmonics of both elevations and currents in shallow water regions are
13 modified by the presence of the surge. By this means it is possible to understand why a surge
14 residual in shallow water determined by de-tiding a surge event using a tidal prediction based
15 upon a long tidal time series still contains energy at tidal frequencies. In addition the extent
16 of modification of tidal constituents in shallow water depends upon location and wind
17 direction and the processes determining this are also considered.

18 In essence the objective of this paper is to use a finite element model, namely
19 TELEMAC (Nicolle and Karpytchev 2007, Fernandes et al 2002, 2004, Heniche et al 2000)
20 with an unstructured grid covering the west coast of Britain to examine to what extent strong
21 winds, comparable to those that occur during storm surges, modify the fundamental and
22 higher harmonics of the tide in shallow water. As such it extends the work of Jones and
23 Davies (2007a) who only examined the surge.

24 The sea region off the west coast of Britain is chosen because it has been the focus of
25 a detailed study over a number of years of processes influencing storm surges in the region

1 (e.g. Lennon 1963, Heaps 1983, Davies and Lawrence 1995, Davies and Jones 1992, 1996,
2 Jones and Davies 1998, 2001, 2003a,b). Furthermore the area covers a range of water depths,
3 with deep water areas (depth of up to 150 m) to the north off the west coast of Scotland, and
4 the North Channel. In addition there are comparable water depths in the Celtic Sea and St.
5 George's Channel (Fig. 1). Storm surges generated outside the area of the model and in these
6 deep water regions are intensified as they propagate into the eastern Irish Sea (Figs. 1,2)
7 where water depths are much shallower (on average of order 25 m, see Fig. 2). In the
8 shallow eastern Irish Sea, there is significant tide surge interaction, and in shallow coastal
9 regions "wetting and drying" occurs, depending upon the state of the tide and the intensity of
10 the surge. Since these highly non-linear processes are a maximum in the eastern Irish Sea
11 this paper focuses upon how surge effects modify the tides in these regions.

12 The TELEMAC finite element code with the unstructured grid given in Fig. 3 was
13 used in the calculations since an accurate tidal solution was obtained previously (Jones and
14 Davies 2005, 2006, 2007b). In addition the fine mesh in this model in the eastern Irish Sea
15 enables an accurate representation of interaction in this region to be modelled. The model
16 also incorporates "wetting and drying" algorithms (see Balzano 1998 for a review of methods
17 used in finite element models) that allow for an accurate solution in near coastal regions. The
18 ability of the finite element method to enhance the mesh in near coastal regions (e.g. Jones
19 2002, Walters 2005, Werner 1995, Legrand et. al. 2006, Levasseur et. al. 2007 and reviews
20 by Greenberg et. al. 2007, Legrand et. al. 2007)) makes it ideal for modelling studies such as
21 the present one.

22 A brief description of the working equations is presented in the next section, with
23 subsequent sections dealing with the influence of orthogonal components of the wind stress
24 upon the M_2 tide and its higher harmonics. The main findings of the study are summarized in
25 a final section.

1 2. THE HYDRODYNAMIC EQUATIONS AND MODEL FORMULATION

2 Following earlier work the domain of the region is identical to that of Davies and
 3 Jones (1992) (hereafter DJ92) and Jones and Davies (2005, 2006), and extends over a range of
 4 latitudes. Following this work the two-dimensional form of the hydrodynamic equations in
 5 polar coordinates is solved, namely

6
$$\frac{\partial \zeta}{\partial t} + \frac{1}{R \cos \phi} \frac{\partial}{\partial \phi} V \cos \phi + \frac{1}{R \cos \phi} \frac{\partial}{\partial \chi} U = 0 \quad (1)$$

7
$$\frac{\partial U}{\partial t} + S_u - 2\omega \sin \phi V = \frac{-g}{R \cos \phi} \frac{\partial \zeta}{\partial \chi} + \frac{\tau_\chi^s - \tau_\chi^b}{\rho (h + \zeta)} \quad (2)$$

8
$$\frac{\partial V}{\partial t} + S_v + 2\omega \sin \phi U = \frac{-g}{R} \frac{\partial \zeta}{\partial \phi} + \frac{\tau_\phi^s - \tau_\phi^b}{\rho (h + \zeta)} \quad (3)$$

9 where S_u, S_v are the non-linear momentum terms, details of which are given in DJ92.

10 The nomenclature used in these equations is χ, ϕ , denote east longitude, (positive
 11 eastward) and north latitude (positive northward), respectively, h depth below the undisturbed
 12 depth of water, t time, ζ elevation of the sea surface, ρ sea water density, R the radius of the
 13 Earth, ω the angular speed of the Earth's rotation, g the acceleration due to gravity, U, V
 14 eastward and northward components of current, τ_χ^b, τ_ϕ^b , components of bottom stress given
 15 by

16
$$\tau_\chi^b = k\rho U \sqrt{U^2 + V^2}, \quad \tau_\phi^b = k\rho V \sqrt{U^2 + V^2} \quad (4)$$

17 with k a coefficient of bottom friction, fixed at $k = 0.0025$. At the sea surface the wind stress
 18 components τ_χ^s, τ_ϕ^s are specified.

19 The horizontal gradient normal to the coast of alongshore velocity was taken as zero.
 20 In shallow water areas “wetting” and “drying” can occur within the tidal cycle. Various
 21 options exist in the literature for doing this (see Ip et al. 1998, Fortunato et al 1997, 1999,
 22 Heniche et al 2000 for a discussion of these). The TELEMAC code option of removing the

1 terms in the hydrodynamic equations which became physically unrealistic was used in the
2 calculations. This is consistent with methods used in finite difference models Flather and
3 Hubbert (1989) and also by Jones and Davies (2006). In the finite element model in shallow
4 water regions where significant “wetting and drying” occurs energy is lost to higher
5 harmonics. At a closed boundary the normal component of velocity was set to zero. The
6 open boundary M_2 tidal forcing was identical to that used by Jones and Davies (2006,
7 2007a,b). In essence only the M_2 tide was specified along this boundary, and its higher
8 harmonics were generated by non-linear effects within the region. A detailed comparison at a
9 significant number, of order 100 coastal and off-shore gauges (including those used here in
10 subsequent tables) showed that the model could accurately reproduce the fundamental and
11 higher harmonics of the tide in the region (see Jones and Davies 2005, 2007b for details of
12 tide gauge locations and model accuracy). In the wind forced calculations only tidal forcing
13 was applied along the open boundary, and hence any external surge effects entering the
14 region were excluded. (A detailed discussion of external surge influence during a specific
15 surge, namely November 1977 can be found in Davies and Jones (1992), although in the
16 shallow eastern Irish Sea local wind forcing dominates over the external surge). The neglect
17 of external surge forcing, which varies significantly from one surge to another, is consistent
18 with the aim of investigating how the tide in shallow water is modified by uniform wind
19 forcing over the region. Solutions were determined in all cases by integrating forward in time
20 from a zero initial state over eight tidal cycles with both tidal and wind forcing. A detailed
21 examination of time series at various locations (see later) showed that a periodic tidal and
22 steady surge response had been achieved by the fourth tidal cycle.

23 The final tidal cycle was then harmonically analysed to determine the amplitude and
24 phase of the M_2 tide and its higher harmonics. Differences between these analyses for a
25 range of wind directions, and those derived from a calculation with only tidal forcing are used

1 to quantify how the surge has modified the tide. The steady state surge residual was
2 computed as the residual from this harmonic analysis and hence did not contain any energy at
3 the tidal frequencies. In essence the surge was derived by “de-tiding” the total using tidal
4 constituents obtained from this harmonic analysis, and not from a “tide only” calculation. In
5 order to understand the role that wind direction plays in modifying the tide, surge elevations
6 obtained by de-tiding using the tidal constituents derived at the time of the surge are also
7 presented.

8 3. NUMERICAL CALCULATIONS

9 In order to examine how storm surges influence the tide, calculations were performed
10 with a steady wind stress of 1.0 Pa, corresponding to the strong wind forcing that occurs
11 during a surge. Initially (Calc 1, Table 1) a wind stress from the west was examined.
12 Subsequently an orthogonal wind stress from the north (Calc. 2) was used. In a final
13 calculation to determine the degree of linearity in the response of the tide, a wind from the
14 south (Calc 3) was applied. In a linear system the response should be the negative of that
15 computed with the north wind. In addition to examining the effect upon the tide, the spatial
16 variability of the surge over the eastern Irish Sea is considered. This was done in order to
17 understand how changes in total water depth due to the surge influenced the various tidal
18 constituents. As shown by Jones and Davies (2007a), in order to accurately compute the
19 surge it is necessary to use a tidal solution derived from an harmonic analysis of the tide and
20 surge at the time of the surge. This approach was used here. By comparing changes in tidal
21 harmonics in different regions produced by the addition of meteorological forcing in different
22 directions then the importance of spatial variations in non-linear effects upon the tide can be
23 quantified.

24 3.1 Effect of a westerly wind stress of 1.0 Pa upon the tide

1 Since the major effect of the storm surge upon the tide occurs in shallow water
2 regions, the focus will be the eastern Irish Sea, although the model computes the response
3 over the whole domain. Before examining the effect upon the tide it is valuable to examine
4 the storm surge elevation distribution over the eastern Irish Sea.

5 It is evident from the surge elevations, (derived by de-tiding the total elevation as
6 described previously), presented in Figs. 4 and 5 that the response of the region to westerly
7 wind forcing, namely onshore winds in the eastern Irish Sea is an increase in elevation in this
8 region. A decrease in elevation occurs in the Celtic Sea (not shown), as wind forces water
9 into the eastern Irish Sea. The rise in sea level from west to east across the eastern Irish Sea,
10 rapidly increases as the water shallows. This can be readily understood in terms of the wind
11 stress forcing term $\tau_x/(h + \zeta)$ which for a uniform wind stress τ_x , increases as the water
12 shallows. The rapid rise in water level in the nearshore estuarine regions (namely Solway,
13 Morecambe Bay and Liverpool Bay (see Figs. 1, 2 for locations)) of the eastern Irish Sea is
14 clearly evident in Figs. 4 and 5 with water levels increasing, in shallow water to values
15 exceeding 0.3 m as the coast is approached. In the nearshore region there is significant small
16 scale variability due to changes in topography and “wetting and drying” occurring during the
17 tidal cycle. Although the present finite element mesh is sufficiently fine to resolve the
18 dominant features of these small scale variations, in some very nearshore regions, a finer
19 mesh would be valuable. However without accurate bathymetry data to match this refined
20 mesh, solution accuracy would still be limited.

21 To understand how the presence of the surge changes the tide due to non-linear
22 interaction and enhanced bottom stress due to surge current (see later), it is necessary to
23 compute changes in tidal amplitude ΔA and phase Δg derived as the difference between tidal
24 amplitude and phase from the harmonic analysis of a tide and surge solution, minus those
25 from the tidal solution. Contours of ΔA in cm, and Δg (not shown but comparable for the

1 M_2 , M_4 and M_6 tidal constituent in the west wind case), in shallow coastal regions of the
2 eastern Irish Sea illustrated here in terms of Morecambe Bay and Liverpool Bay are given in
3 Figs. 6 and 7. It is evident from Fig. 6a that in the shallow northern part of Morecambe Bay,
4 the effect of the wind from the west has been to increase the amplitude derived by harmonic
5 analysis of tide and surge time series of the M_2 tidal elevation by up to 30 cm. From Fig. 5 it
6 is apparent that the storm surge increases water levels in this area by up to 40 cm, which will
7 tend to reduce tidal damping due to bottom friction. This will be discussed later in the
8 context of time series of specific terms in the hydrodynamic equations at selected points. In
9 addition some regions which were “wet and dry” during a tidal cycle will remain “wet” due
10 to the presence of the surge. Although M_2 tidal elevation amplitude increases in the north of
11 Morecambe Bay (namely north of $54^\circ 06'$, Fig. 6a), it is evident that in the nearshore region
12 to the south of this, there is a decrease in amplitude of up to -10 cm. The reason for this is
13 not entirely clear, (but is discussed later in terms of time series), although it does coincide
14 with the area of maximum surge elevation of up to 50 cm (Fig. 5). One possible explanation
15 is that since bed stress is given by $k u |u| / (h + \zeta)$, then its reduction due to increase in $(h +$
16 $\zeta)$ may be negated by an increase in $u |u|$ due to strong surge currents in shallow water.
17 This will give rise to significant spatial variability. As shown in Figs. 6b and 6c any local
18 changes in bed stress can lead to significant small scale changes in the difference in
19 amplitude of both the M_4 and M_6 tidal elevations between those computed with tide and surge
20 and tide only, which increase/decrease in some areas. Since both of these constituents are
21 influenced by the regional extent of “wetting and drying”, changes in bed stress and
22 momentum advection produced by the presence of surge elevations and currents, small scale
23 variations may be expected (see later discussion). It is important to note that Figs. 6a, 6b and
24 6c, are differences in amplitude of the M_2 , M_4 and M_6 tidal elevations due to the presence of
25 the surge. In the case of M_6 , the contour interval is 1 cm, and hence shows significant small

1 scale variability, in the difference. As discussed previously a refined mesh and more accurate
2 bottom topography would be required to improve the accuracy of the solution. However, all
3 figures do show that the tide has been appreciably influenced by the presence of the surge.
4 Consequently when a surge residual is determined by de-tiding using a tide only solution the
5 true tidal signal at the time of the surge is appreciably different and hence some tidal energy
6 will remain in the surge derived by this method.

7 A similar picture to that found in Morecambe Bay occurs in the Liverpool Bay and
8 entrance to the Mersey region (Fig. 7a-c). It is interesting that in the region at the entrance to
9 the Mersey and just outside it, M_2 tidal amplitude decreases by -10 cm, in the area of
10 maximum surge amplitude (Fig. 4) in a similar manner to that found in Morecambe Bay.
11 Elsewhere in the coastal region, the M_2 tidal amplitude shows small scale decreases and
12 increases. As in Morecambe Bay the higher harmonics, namely M_4 and M_6 have appreciable
13 small scale variability in the region (Figs. 7b and 7c). As in Morecambe Bay, the accuracy of
14 these small changes in higher harmonics would be enhanced by a finer mesh and more
15 detailed bottom topography. To complete this study of the large scale effects of a westerly
16 wind upon the tide a detailed point comparison is given in Tables 2a-c at shallow water
17 locations in the eastern Irish Sea shown in Fig. 2.

18 At positions such as Hilbre, Conwy and Barrow which are adjacent to regions of
19 shallow water it is difficult to determine which nodal point in the finite element grid is most
20 appropriate for the comparison. Also there is no nodal point which is exactly located at
21 Hilbre or Barrow. For this reason and to determine tidal spatial variability in the region, the
22 tidal amplitude and phase at nodal points a distance Δ from the port are given in Tables 2a-c.
23 To understand the influence of local water depth h , this is also presented. At other locations
24 namely Liverpool P.P, Liverpool Bay and SN35 situated in deeper water there is little or no

1 variability over distances of order 4 km from the gauge, and hence only the solution at the
2 nearest node is given.

3 From Figs. 6a and 7a and Table 2a, it is apparent that away from the near coastal
4 region of the eastern Irish Sea the decrease in M_2 tidal amplitude due to the presence of the
5 west wind is of the order of 4 cm with phase changing by about 1° (e.g. SN35, $h = 33.3$ m,
6 $\Delta A = 4$ cm, $\Delta g = 1^\circ$, Table 2a). However, as water shallows in the Liverpool Bay region,
7 there is a continuing decrease in amplitude due to the presence of west wind forcing (e.g.
8 Liverpool Bay, $h = 11.2$ m, $\Delta A = 6$ cm, Liverpool P.P, $h = 8.2$ m, $\Delta A = 14$ cm, Table 2a),
9 although there is little phase change. In shallow water regions such as Hilbre water depth
10 changes from 16.2 m to 2.0 m over distances of the order of a kilometre (Table 2a).
11 Associated with these changes in water depth are variations in M_2 tidal amplitude from 275
12 cm to 324 cm, although phase change is of the order of 1° (Table 2a). The effect of forcing
13 with a westerly wind is to increase water depth in this region. Consequently in very shallow
14 regions, namely $h = 2.0$ and 2.3 m the increase in water depth reduces the effect of bottom
15 friction and hence tidal amplitude increases from 275 cm to 291 m ($h = 2.0$ m) and 294 cm to
16 306 cm ($h = 2.3$ m). At deeper water locations namely $h = 9.6$ m and 16.2 m, as discussed
17 previously for SN35 and Liverpool, the increase in bed stress due to stronger storm surge
18 currents, offsets its decrease due to an increase in water depth, and M_2 tidal amplitudes
19 decrease (319 cm to 309 cm, ($h = 9.6$ m), and 324 cm to 314 cm, $h = 16.2$). However, as
20 found at deeper water sites there is little phase change. This comparison clearly shows why
21 at a port such as Hilbre where there is a substantial depth change over distances of order 1
22 km, the change in the M_2 tide due to the addition of a westerly wind stress shows such small
23 scale variability.

24 At a port such as Conwy which is surrounded by shallow water the addition of a
25 westerly wind leads to an increase in M_2 tidal amplitude at all locations in the vicinity of

1 Conwy (Table 2a). As previously there is no substantial change in tidal phase. At Barrow RI
2 and HP, again in shallow water the addition of a westerly wind tends to increase M_2 tidal
3 amplitude, although in a water depth of order 9 m there is no change. This suggests that
4 depending on the exact location of such points, the increase in bed stress due to the enhanced
5 current of tidal origin is offset by its decrease due to change in total water depth.

6 This detailed examination explains why de-tiding using a tide only solution fails to
7 remove all tidal energy from the surge. As shown here, in deep water this is not substantially
8 different from that computed with the tide only and hence a linear decomposition into tide
9 and surge is valid, and a linear subtraction of the tide is possible. However, in shallow
10 regions non-linear effects and enhancements in bottom stress due to the presence of storm
11 surge currents, modify the tidal amplitude, leading to small scale increases and decreases in
12 tidal amplitude. This explains the small scale variability in shallow water shown in the M_2
13 ΔA plots given in Figs. 6a and 7a. In addition it is in part the reason for the small scale
14 variations in near-shore surge elevation shown in Figs. 4 and 5.

15 Besides the west wind influencing the M_2 component of the tide, it also affects the M_4
16 component as shown in the ΔA distribution (Figs. 6b and 7b). Although this component in
17 offshore regions is significantly smaller than the M_2 tide, it is evident (Table 2b), that at
18 SN35, and Liverpool Bay there is a slight change with a reduction of over 6 cm at Liverpool
19 P.P (Table 2b). Unlike the M_2 tide an appreciable change occurs in the phase (Table 2b). In
20 shallow regions such as Hilbre, not only does the M_4 tide change over small distances, but
21 there is a major change (of order 60°) in its phase (Table 2b). The addition of the west wind
22 appears (Table 2b) to increase amplitude and phase in deeper water ($h = 9.6$ and 16.2 m),
23 with a decrease in shallow water (Table 2b). This also occurs at Conwy which is situated in
24 shallow water where at all locations M_4 amplitude and phase decrease with the addition of the
25 westerly wind. However, the response to westerly wind forcing is rather different at Barrow

1 where in very shallow water denoted by $h = 0.0$ m in Table 2b, the M_4 amplitude increases
2 with little change in phase, whereas in deeper water there is little change in amplitude
3 although some in phase. These results explain the small scale variation shown in Figs. 6b and
4 7b.

5 In deeper water regions, namely SN35 and Liverpool Bay the M_6 tidal amplitude is of
6 the order of 5 cm, or less (Table 2c). In shallower water regions namely Liverpool P.P it
7 reaches the order of 15 cm, although it is not significantly affected by the west wind. At
8 Hilbre in deeper water ($h = 9.6$ and 16.2 m) there is a slight increase in amplitude with a
9 decrease in phase. In shallow water (h of order 2 m), the amplitude decreases by 50% with
10 an associated change in phase. However at Conwy in comparable water depths the change is
11 much less and does not follow a consistent picture. A consistent change depending on water
12 depth between M_6 tidal amplitude with and without a westerly wind was not evident at
13 Barrow RI or HP. This high degree of spatial variability in the change in M_6 tidal amplitude
14 in shallow water is clearly evident in Figs. 6c and 7c.

15 3.2 Effect of a northerly wind of 1.0 Pa upon the tide

16 In a subsequent calculation (Calc. 2, Table 1) the model was forced by a northerly
17 wind stress. The steady-state surge residual (Figs. 8 and 9) showed a decrease (negative
18 surge) over the majority of the region (Fig. 8). A southerly wind, considered later, showed a
19 positive surge (Fig 10). For the northerly wind a negative surge of increasing magnitude
20 occurred in the Solway and Morecambe Bay as the northern edge of these regions was
21 approached, as a result of the local wind stress in these areas. In the coastal region in
22 particular in Morecambe and Liverpool Bays there is significant spatial variability in the
23 surge elevation. This in part arises from changes in topography but is also due to the
24 influence of the wind upon the tide as shown in the ΔA contours (Figs. 11 and 12), and the
25 port values given in Tables 2a-c. As discussed previously, the accuracy of the small scale

1 variability shown in Figs. 11 and 12, would be improved by more accurate bottom
2 topography and a refined nearshore mesh.

3 It is evident from Figs. 11a and 12a and Table 2a, that at deep water locations (e.g.
4 SN35 and Liverpool Bay, Table 2a) the M_2 tidal amplitude is reduced by 4 cm, by the
5 presence of the northerly wind. This is comparable to that due to the westerly wind,
6 suggesting that it is frictional effects due to the increase in currents rather than changes in
7 surge elevation, which are different in the two cases, that are responsible for this. This point
8 will be considered later in connection with time series of various terms in the hydrodynamic
9 equations at specific points. In shallower water, namely Liverpool P.P, although tidal
10 amplitude decreases (see Fig. 12a and Table 2a), this decrease is not as large as for the west
11 wind case. This will be examined later in terms of additional bed stress due to surge currents,
12 which has the effect of decreasing the tidal amplitude. At Hilbre, in deeper water locations in
13 the area, namely $h = 9.6$ m and 16.2 m the tidal amplitude decreases by about the same
14 amount as in the west wind case (Table 2a). In addition in shallow water $h = 2$ m and 2.3 m,
15 a 10 cm decrease is also evident. This shallow water response is different from the west wind
16 case where M_2 tidal amplitudes increased in shallow water, due to the presence of the wind.
17 Differences in the spatial distribution of ΔA contours are clearly evident from a comparison
18 of Figs. 7a and 12a. Similar differences occur in Morecambe Bay (compare Figs. 6a and
19 11a). In the west wind case the water level increased in the regions and hence the effect of
20 bed stress was reduced and tidal amplitude increased. In the present case water depths
21 decrease, hence bed stress increases and tidal amplitude decreases.

22 At Conwy, in shallow water, the tidal amplitude in the north wind case is reduced at
23 all locations (Table 2a). Similarly at Barrow RI and HP, M_2 tidal amplitude in shallow water
24 regions decreases with the addition of the northerly wind stress. This is the opposite to that
25 found with a westerly wind stress. This detailed study explains why ΔA for the M_2 tide

1 (Figs. 11a and 12a) varies significantly over short distances and in many regions has the
2 opposite sign to that found with a westerly wind stress.

3 As for the westerly wind case, ΔA for the M_4 tide computed with northerly wind
4 forcing shows significant spatial variability in the nearshore region (Figs. 11b and 12b). In
5 Morecambe Bay the change in the M_4 tide produced by the north wind (Fig. 11b) is
6 significantly larger than that produced by the west. This is due to the fact that the north wind
7 leads to a reduction in water level and hence an increase in the shallow water terms that give
8 rise to the M_4 and M_6 tide (see later discussion in terms of time series). In addition in areas
9 where “wetting and drying” occur, at times of low water when drying is present, the tidal
10 elevation time series is limited by the water depth and is no longer truly sinusoidal (see later
11 discussion). A consequence of this is the harmonic analysis of such a time series contains
12 energy in the higher harmonics due to the “Gibbs phenomenon” associated with the period of
13 drying (Hall and Davies 2005). A more detailed discussion of this in terms of time series is
14 given later. Similar differences between westerly and northerly wind effects upon the M_4 tide
15 are found in the shallow water regions of Liverpool Bay (compare Figs. 7b and 12b). From
16 Table 2b it is apparent that even at deeper water locations such as Liverpool Bay and
17 Liverpool P.P. the M_4 tidal amplitude and phase increase by about 5 cm and 20° when a
18 northerly wind is added. A very similar increase occurs at the deeper water locations at
19 Hilbre, with a substantially larger increase in amplitude but little change in phase in the
20 shallower locations around the Hilbre gauge. An increase in elevation and phase, in deeper
21 regions ($h = 9.1, 6.4, 5.9$ m) occurs at Barrow, although in the shallow regions ($h = 0.0$ m)
22 there is a small decrease in elevation amplitude with little change in phase. This change in
23 M_4 elevation amplitude at Barrow is the opposite of that found with the westerly wind. In the
24 westerly wind case water levels rose in the region. Consequently in very shallow regions
25 bottom frictional effects were reduced leading to an increase in M_4 tidal amplitude. In the

1 present case they are reduced by the northerly wind. The differences in ΔA over the short
2 distance between shallow and deeper water, explains the spatial variability seen in Figs. 11b
3 and 12b.

4 For the M_6 component (Figs. 11c and 12c), there is a small increase in amplitude at
5 SN35 as for the west wind case, although a decrease in Liverpool Bay rather than the increase
6 found with the west wind. At Hilbre there is only a small change in amplitude and phase
7 compared to the large change with the west wind. As discussed previously the west wind in
8 this region increases water levels thereby reducing bottom stress which is a major source of
9 M_6 (see later discussion in terms of time series). In the present case there is a reduction in
10 water level (Fig. 8), although this is small 0.2 m, in Liverpool Bay which explains the small
11 change in M_6 with the north wind in this region. However, it is larger further north with
12 values of the order 0.5 m in Morecambe Bay (Fig. 9). This reduction in water level explains
13 the significant change in M_6 tidal amplitude in this region (Fig. 11c).

14 At Barrow RI and HP there is a general reduction in water level of 0.5 m, with
15 significant local variation giving a decrease of 0.8 m in some areas. In the very shallow
16 water regions ($h = 0.0$ m) there is a significant increase in M_6 tidal amplitude from the order
17 of 5 cm to 18 cm (Table 2c). This is probably due to an increase in bottom friction and
18 drying during the tidal cycle which has the effect of increasing the M_6 tide (see later
19 discussion). This change in ΔA (M_6) is very different from the west wind case, which raised
20 water levels in this region producing a slight reduction in M_6 . The substantial difference in
21 ΔA values for the M_6 tide both in amplitude and spatial distribution in Morecambe Bay
22 between the westerly and northerly winds is clearly evident from a comparison of Figs. 6c
23 and 12c. Similar differences although to a lesser extent are evident in the coastal regions of
24 Liverpool Bay (Figs. 7c and 12c). This clearly shows that ΔA values change from one
25 location to another over quite small distances and depend upon wind stress direction.

1 3.3 Effect of a southerly wind of 1.0 Pa upon the tide

2 To examine to what extent wind direction influenced the solution, the previous
3 calculation was repeated with the same wind stress from the south (Calc 3, Table 1). By this
4 means the extent to which the response can be linearly scaled with the wind field can be
5 determined. If the response is truly linear then the surge elevation determined with a
6 southerly wind (Fig. 10) should be the negative of the northerly wind solution. Similarly
7 there should be a corresponding change in the distribution of ΔA .

8 The large scale features and magnitude of the surge elevation in deep water (not
9 shown) were comparable to those found with the northerly wind stress, with elevations,
10 having the opposite sign. Similarly, in shallow water regions such as the eastern Irish Sea
11 (compare Fig. 10 and Fig. 8) away from shallow coast regions the distributions had the same
12 features, with elevations of the opposite sign. This suggests that when the surge is de-tided
13 using tidal harmonics computed at the time of the surge, the resulting surge scales in a linear
14 manner with the imposed wind stress. However as before the surge changes the tide in
15 shallow water regions as shown in Figs. 13 and Fig. 14, and in Table 2. However these
16 changes in the tide have a different spatial distribution and amplitude from those computed
17 with a northerly wind stress (compare Figs. 13, 14 and 11, 12). For the M_2 tide at location
18 SN35 in deeper water it is apparent that the southerly wind decreases M_2 tidal amplitude
19 more than the northerly. This is probably due to frictional effects arising from larger surge
20 currents produced by southerly more than northerly winds (see later discussion).

21 However in Liverpool Bay both wind stresses give the same reduction, whereas at
22 Liverpool P.P. the northerly wind reduces the M_2 tidal amplitude more than the southerly
23 (Table 2a). These changes in M_2 tidal amplitude with the addition of winds from different
24 directions, reflect changes in the M_2 co-amplitude lines in the region, due to modification of
25 water depth and bottom friction over the whole region produced by the surge.

1 In shallow water regions such as Hilbre and Conwy the southerly wind produces a
2 small change in sea level (Fig. 10) with an associated small change in M_2 tidal amplitude
3 (Table 2a). At Barrow RI and HP, the southerly wind gives rise to a local increase in water
4 level (Fig. 10). In very shallow water $h = 0.0$ m, this gives rise to an increase in M_2 tidal
5 amplitude by about 30 cm. In these regions the increase in bed stress due to enhanced wind
6 forced current is offset by its reduction due to increase in water depth. However, in deeper
7 water $h = 9.1, 6.4, 3.3$ m, elevations are reduced due to the enhanced flow. Although the
8 change ΔA in M_2 tidal amplitude due to the north wind has on average the opposite sign to
9 the south wind case, it is evident from Table 2a, and differences in the spatial distributions
10 given in Figs. 12a and 14a, that there are significant differences in the magnitude of these
11 changes and their spatial variability.

12 From Table 2b, it is apparent that at Liverpool Bay and Liverpool P.P. the M_4 tidal
13 amplitude decreases by 4 cm due to the presence of the south wind. This is comparable to the
14 order of 5 cm increase due to the North wind. At Hilbre in deeper water $h = 9.6$ and 16.2 m,
15 the M_4 amplitude decreases by about 4 cm, with a significantly larger decrease of about 8 cm
16 in shallow water. Although this is in the opposite sense to that found for the north wind, the
17 magnitude of the change is slightly different, namely about 6 cm in both shallow and deep.
18 Although these magnitudes are different, the fact that the change in M_4 is in the opposite
19 direction and of comparable magnitude for each wind direction suggests some linearity in its
20 response. Similarly at Conwy in shallow water the south wind produces a change of M_4 tidal
21 amplitude of comparable magnitude to the north wind but in the opposite sense.

22 In deeper water at Barrow RI and HP, a decrease in M_4 amplitude with the southerly
23 wind, with an increase due to the northerly wind is evident. However, in shallow water $h =$
24 0.0 , a decrease is evident for both wind directions. This suggests that for M_4 there is some
25 degree of linearity in the change ΔA for different wind directions provided the water is not

1 too shallow. However in very shallow regions such as Morecambe Bay, it is evident that the
2 distribution of ΔA contours of the M_4 tide computed with the south wind (Fig. 13b) is
3 substantially different from that computed with the north wind (Fig. 11b). Although in the
4 southwind case there is a reduction in M_4 amplitude, with on average an increase in the north
5 wind case due to decrease in water depth, these do not scale with the wind stress magnitude.
6 Similar differences in ΔA distributions and values are found in nearshore regions in
7 Liverpool Bay (compare Figs. 14b and 12b).

8 For the M_6 tide there is on average, particularly in shallow water, (see Conwy, Barrow
9 etc) an increase in amplitude when southerly wind forcing is included. This is consistent with
10 that found for the north wind although at Barrow the change in ΔA for M_6 due to the south
11 wind is less than the north wind. The small scale variability of the change in ΔA for the two
12 different wind directions is reflected in Figs. 11c, 12c and 13c, 14c.

13 This series of calculations clearly shows that in shallow water the tidal constituents
14 are affected by the presence of the wind stress, due to the importance of non-linear effects in
15 these regions. To quantify the extent and regional variation of the linearity of the surge
16 derived by de-tiding using tidal harmonics derived from analysing the tide and surge solution
17 it is valuable to consider the difference between the surge due to the northerly wind and that
18 determined by scaling the southerly wind solution by -1.0. If the response is linear these two
19 solutions should be identical and their difference zero.

20 A plot over the whole model domain (not shown) revealed that this was the case
21 except in the nearshore region, particularly in the eastern Irish Sea. In this area the regions
22 where there was most difference between the two solutions was in the Solway Firth,
23 Morecambe Bay and Liverpool Bay, although on average the difference was below 5 cm.
24 This suggests that the surge residual derived by this method, can be readily scaled to give a
25 residual for an arbitrary steady wind field. In this de-tiding approach, the non-linear

1 interaction mainly appears as a change in the tide and hence the tidal constituents rather than
2 the surge.

3 4. EFFECT OF THE SURGE UPON COMPUTED TIDAL CURRENTS

4 In this section we examine changes in tidal currents in shallow water due to tide-surge
5 interaction for a number of wind directions. This complements the study as to how tide surge
6 interaction modified the amplitude and phase of the M_2 , M_4 and M_6 elevations, by examining
7 to what extent tidal ellipses are modified by the surge. Considering initially the west wind
8 case, distributions of the difference in tidal current ellipse (determined from the difference in
9 tidal current analysis at the M_2 , M_4 and M_6 frequencies, without and with the surge) over the
10 whole region between a tide only solution and that with tide and the westerly wind (not
11 presented) showed that changes were mainly confined to near coastal regions, in particular to
12 the eastern Irish Sea (Figs. 15-19).

13 It is evident from Fig. 15, and expanded plots of Morecambe Bay and Liverpool Bay
14 (Figs. 18a and 19a), that although the M_2 tidal currents are not significantly influenced by the
15 surge in offshore regions there are appreciable changes in shallow water areas. This is
16 consistent with the changes found in M_2 tidal elevation amplitude. In Morecambe Bay it is
17 clear (Fig. 18a) that there is significant spatial variability in the M_2 tidal ellipse difference
18 which is largest in the shallow northern part of the estuary and smallest in the deep south
19 west corner. Similarly in the Liverpool Bay region (Fig. 19a) the largest changes occur in the
20 Mersey and Dee estuaries.

21 The spatial distribution of the change in M_4 tidal current ellipse (Fig. 16) over the
22 eastern Irish Sea is comparable to that found for the M_2 tide. This is to be expected since this
23 component is generated from the M_2 tide by non-linear interaction. However, its magnitude
24 is smaller, reflecting the smaller M_4 tidal currents compared to the M_2 . As for the M_2 tide the
25 change is largest in the northern part of the bay, and negligible in deep water. In the deeper

1 water regions of Liverpool Bay (Fig. 19b) there is no appreciable change in the M_4 tidal
2 currents, although they are significantly modified in the estuarine regions.

3 The M_6 tidal currents which are negligible away from shallow water regions (Jones
4 and Davies 2007b) are essentially unaffected by the surge, except in near coastal regions (Fig.
5 17) where bottom friction is important and “wetting and drying” can occur. Although the
6 change in M_6 currents is small compared to M_4 , it is significant in the shallow northern region
7 of Morecambe Bay (Fig. 18c) and in the Dee and Mersey estuary area (Fig. 19c).

8 Although the detailed patterns and values of the change in tidal current ellipses due to
9 the other wind fields (not presented) are slightly different to those found in the west wind
10 case, the general conclusion that tidal currents are mainly affected by storm surge currents in
11 shallow water remains the same. This suggests that as the nearshore grid is refined in a finite
12 element model to improve near coastal resolution and hence the computed surge, tidal
13 currents will be increasingly modified by the presence of the surge.

14 5. SPATIAL VARIABILITY IN TIME SERIES OF TERMS GIVING RISE TO TIDE- 15 SURGE INTERACTION

16
17 In the previous sections the spatial variability of the change in tidal elevation
18 amplitude and current ellipse distributions at the M_2 tidal frequency and its higher harmonics,
19 due to the presence of the wind was examined. This change in tidal amplitude is in part
20 produced by an increase/decrease in water depth, particularly in shallow water where drying
21 can occur. In addition changes in the non-linear bottom friction terms $ku(u^2 + v^2)^{1/2}/(h + \zeta)$
22 and $kv(u^2 + v^2)^{1/2}/(h + \zeta)$, and non-linear momentum advection terms udu/dx , vdu/dy , udv/dx
23 and vdv/dy which in shallow water couple together tidal and surge currents, namely tide-
24 surge interaction also influence the distribution of energy between tidal constituents and the
25 surge. In this section by examining time series of these various terms their importance in
26 deep and shallow locations, and their influence on tide-surge interaction can be appreciated.
27 To this end time series over cycles 7 and 8 (the final two tidal cycles) at locations A in deep

1 water (Fig. 2), and B in the shallow water region of Morecambe Bay (Fig. 2), are examined in
2 detail for the cases of the southerly wind, leading to an increase in water level, and northerly
3 wind leading to a decrease in water level.

4 Considering initially the elevation time series at position (A) due to the tide only and
5 tide and surge, it is evident from Fig. 20, that in the absence of wind forcing, tidal elevation
6 has a mean value of zero, with an amplitude of about 2.7 m, and energy is confined to the M_2
7 period. These values were confirmed by a harmonic analysis of the time series. In the case
8 of a southerly or northerly wind, mean sea level, increased/decreased by about 0.2 m, with
9 the tide remaining unchanged. Time series of the non-linear friction and advective terms at
10 this location (not presented) showed that they were small and their change, taken as the
11 difference between tide and surge and tide only, namely Fig. 21 (frictional effects) and Fig.
12 22 (advective terms) revealed only small changes depending upon the direction of wind
13 forced currents compared to tidal currents, and in addition the small change in water depth in
14 the bottom friction case. In essence in deep water the steady state balance was between wind
15 stress and sea surface elevation gradients with the non-linear terms playing little or no role.
16 Consequently the M_2 tide dominated the solution, with total elevations and currents
17 determined as a linear combination of those due to tidal and wind forcing. In essence non-
18 linear coupling due to tide-surge interaction was negligible.

19 In shallow water (Position B, Fig. 2) due to “wetting and drying” the tidal elevation
20 curve (Fig. 23) shows significant asymmetry. Although the maximum elevation exceeds 3 m,
21 its minimum value cannot fall below -1.8 m, as this is the water depth in the region, and
22 drying occurs as shown in the time series (Fig. 23). As demonstrated by Hall and Davies
23 (2005) when such an asymmetric time series is harmonically analysed besides energy
24 occurring at the M_2 period, it is also present at its higher harmonics.

1 In the case of a southerly or northerly wind stress the water depth increases/decreases
2 in the region thereby changing the asymmetry in the tidal curve (Fig. 23) and hence
3 influencing the amplitude of the M_2 tide and its higher harmonics. Besides the change in sea
4 level produced by the wind, it also influences the time series of the quadratic bottom friction
5 and momentum advection terms (not shown) which are significant in this region. Comparing
6 time series of the difference in these terms derived as previously, namely Figs. 24 (frictional
7 effects) and Fig. 25 (advection terms) shows that they are significantly larger of order 100 to
8 1000 in the friction terms (compare Figs. 21 and 24) and of order 10 to 100 depending upon
9 location in the momentum advection terms (compare Figs. 22 and 25).

10 It is evident from the time series of the quadratic friction and momentum advection
11 terms, and confirmed by harmonic analysis, that there is significant energy at frequencies
12 corresponding to the fundamental and higher harmonics of the tide in these time series.
13 Consequently changes in these non-linear terms produced by the addition of wind forcing
14 will influence at Posn B both the fundamental and higher harmonics of the tide through tide-
15 surge interaction. As shown here, the extent of this interaction depends on water depth, and
16 clearly increases as water depth is reduced, and tidal and wind forced currents increase.
17 Depending upon the relative magnitude of tidal currents and their orientation and phase
18 relative to the local wind forced current, the temporal and spatial variability of both the
19 frictional and advective terms changes significantly. These changes in frictional and
20 advective terms together with “wetting and drying” explains the high spatial variability in the
21 M_2 , M_4 and M_6 components of tidal elevation and current produced by wind forcing.

22 6. CONCLUSIONS

23 In a previous paper Jones and Davies (2007a) examined the extent to which tide-surge
24 interaction modified the computed surge due to uniform constant wind stresses over the west
25 coast of Britain. Here that work is extended to consider how the tide is modified by the

1 surge. As previously a finite element west coast model is used in these calculations. The
2 finite element mesh in the west coast model is such that a high resolution is obtained in the
3 eastern Irish Sea. By this means it is possible to examine the non-linear interaction between
4 tidal and wind forced motion in shallow nearshore regions. Initial calculations were
5 performed with uniform steady westerly and northerly wind stresses of 1.0 Pa. By using
6 orthogonal winds, if the wind forced response of the region was linear then the response to a
7 uniform wind stress of arbitrary magnitude and direction could be determined by scaling and
8 adding these solutions. A southerly wind stress was also considered to examine if the tide is
9 modified in a linear manner by the presence of the surge.

10 Calculations and analysis of time series of surface elevation and the non-linear terms
11 in deep and shallow regions clearly showed that in shallow water coastal regions there are
12 significant non-linear effects which influence both the computed tidal elevation amplitude
13 and tidal current distributions. A detailed examination of the tide showed that the extent to
14 which the tide is changed by the presence of the surge depends upon location, in particular
15 water depth, and wind direction. In shallow water the change in the tide was found to be
16 appreciable and was produced by changes in “wetting and drying”, non-linear bottom
17 friction, and the momentum advection terms due to the presence of the wind. Changes in
18 these terms showed significant temporal and spatial variability depending upon water depth,
19 and alignment of tidal and wind forced currents. Consequently the tide showed appreciable
20 small scale variability in its change produced by wind forcing. The effect of the change in
21 tidal magnitude produced by the wind is that de-tiding a tide and surge calculation using tidal
22 constituents from a tide only solution would lead to energy in the surge in shallow near
23 coastal regions, at tidal frequencies. Such an artificial leakage of energy is found when
24 observed surge elevations are de-tided using a harmonically predicted tide, confirming that
25 the surge does influence the tidal signal. The artificial leakage gives rise to semi-diurnal

1 oscillations in the surge. These have been observed not only in regions such as the Irish Sea
2 but elsewhere (e.g. North Sea Horsburgh and Wilson (2007) and north-west Atlantic, e.g.
3 Bernier and Thompson (2006)), although a detailed study using a numerical model of the
4 form used here has not previously been undertaken.

5 In the present calculation since only M_2 tidal forcing and a steady wind stress was
6 imposed the influence of the surge upon the M_2 tide and its harmonics could be determined
7 by harmonically analysing a short duration (namely a M_2 period) time series. Although this
8 gave significant insight into the effects of the surge upon the various tidal constituents it is
9 difficult to extend to a time varying wind of surge period and larger number of constituents
10 (e.g. M_2 , S_2 , N_2 , K_1 , O_1 Jones and Davies 1998). The major difficulty in this case is that the
11 storm surge only has a short duration of order 2 days. As shown by Hall and Davies (2005)
12 separation of the M_2 and S_2 tide from each other is possible using short periods (of order a
13 few days) output from tide only numerical model runs, due to the absence of noise in model
14 calculations. However, in a storm surge model where meteorological effects are present an
15 accurate separation would be difficult to achieve. Consequently de-tiding the tide and surge
16 calculation using harmonic analysis to determine tidal constituents at the time of the surge
17 would be prone to error in a storm surge simulation model. Also the method of predicting
18 total water levels produced by a surge, namely by adding tidally predicted elevations (based
19 on the harmonic analysis of a long time series at a port) to a surge elevation computed by a
20 numerical model is also prone to error particularly in shallow regions. Consequently in
21 future high resolution nearshore models it will be necessary to use the model to predict the
22 total water level during the surge period. In this case it will be necessary for the model to
23 accurately reproduce the tide in shallow water. However, as model grids in nearshore regions
24 are refined the ability of the model to reproduce tides in these regions is enhanced provided
25 accurate bathymetry is available to match the reduction in mesh size.

1 Although extensive coastal and offshore tidal data sets exists to validate the accuracy
2 of tidal simulations (e.g. Jones and Davies 2005, 2007b), no comparable tidal data sets exist
3 at the time of major surge events to see to what extent the tide has been modified by the
4 surge. If however extensive offshore tide gauge measurements could be made in a region
5 such as Morecambe Bay for a significant number of surge events, and analysed by grouping
6 together surge events occurring under similar wind directions (e.g. westerly, northerly,
7 southerly) some indication of how the tide is modified by the surge and its spatial variability
8 could be obtained. Until such measurements are available for model validation, the most
9 compelling evidence that the surge influences the tide is the presence of significant tidal
10 energy in the surge record when it is derived by de-tiding using a tide derived from a long
11 term record which does not take account of this interaction.

12 ACKNOWLEDGEMENTS

13 The origin of the TELEMAC system is EDF-LNHE and is therefore © EDF-LNHE. Thanks
14 are due to Andrew Lane for providing accurate Mersey bathymetry. The authors are indebted
15 to R.A. Smith for help in preparing diagrams and L. Parry for typing the paper.

16

1 REFERENCES

- 2 Balzano, A. (1998) Evaluation of methods for numerical simulation of wetting and drying in
3 shallow water flow models. *Coastal Engineering*, 34, 83-107.
- 4 Bernier, N.B. and Thompson, K.R. (2006) Predicting the frequency of storm surges and
5 extreme sea levels in the northwest Atlantic. *Journal of Geophysical Research*, 111,
6 C100009, doi10.1029/2005JC003168.
- 7 Bobanovic, J., Thompson, K.R., Desjardins, S. and Ritchie, H. (2005) Forecasting storm
8 surges along the east coast of Canada and the northeastern U.S.: the storm of 21
9 January 2000. *Atmosphere-Ocean*, 44(2), 151-161.
- 10 Davies, A.M. and Lawrence, J. (1995) Modelling the effect of wave-current interaction on
11 the three-dimensional wind driven circulation of the eastern Irish Sea. *Journal of*
12 *Physical Oceanography*, 25, 29-45.
- 13 Davies, A.M. and Jones, J.E. (1992) A three-dimensional wind driven circulation model of
14 the Celtic and Irish Seas. *Continental Shelf Research*, 12, 159-188.
- 15 Davies, A.M. and Jones, J.E. (1996) Sensitivity of tidal bed stress distributions, near-bed
16 currents, over-tides, and tidal residuals to frictional effects in the Eastern Irish Sea.
17 *Journal of Physical Oceanography*, 26, 2553-2575.
- 18 Fernandes, E.H.L., Dyer, K.R., Moller, O.O. and Niencheski, L.F.H. (2002) The Patos
19 lagoon hydrodynamics during an El Nino event (1998). *Continental Shelf Research*,
20 22, 1699-1713.
- 21 Fernandes, E.H.L., Marino-Tapia, I. Dyer, K.R. and Moller, O.O. (2004) The attenuation of
22 tidal and subtidal oscillations in the Patos Lagoon estuary. *Ocean Dynamics*, 54, 348-
23 359.

- 1 Flather, R.A. and Hubbert, K.P. (1989) Tide and surge models for shallow water –
2 Morecambe Bay revisited, pg. 135-166 in Modeling Marine Systems, Vol 1, CRC
3 Press, Boca Raton, Florida, USA.
- 4 Fortunato, A.B., Baptista, A.M. and Luetlich, R.A. (1997) A three-dimensional model of
5 tidal currents in the mouth of the Tagus estuary. *Continental Shelf Research*, 17,
6 1689-1714.
- 7 Fortunato, A.B., Oliviera, A. and Baptista, A.M. (1999) On the effect of tidal flats on the
8 hydrodynamics of the Tagus estuary. *Oceanologica Acta*, 22, 31-44.
- 9 Greenberg, D.A., Dupont, F., Lyard, F.H., Lynch, D.R. and Werner, F.E. (2007) Resolution
10 issues in numerical models of oceanic and coastal circulation. *Continental Shelf*
11 *Research* (in press).
- 12 Hall, P. and Davies, A.M. (2005) The influence of sampling frequency, non-linear
13 interaction, and friction effects upon the accuracy of the harmonic analysis of tidal
14 simulations. *Applied Mathematical Modelling*, 29, 533-552.
- 15 Heaps, N.S. (1965) Storm surges on a continental shelf. *Phil.Trans.R.Soc.*, A257, 351-383
- 16 Heaps, N.S. (1969) A two dimensional numerical sea model. *Phil.Trans.R.Soc.*, A265, 93-
17 137.
- 18 Heaps, N.S. (1983) Storm Surges, 1967-1982. *Geophysical Journal of the Royal*
19 *Astronomical Society*, 74, 331-376.
- 20 Heniche, M., Secretin, Y., Boudreau, P. and Leclerc, M. (2000) A two-dimensional finite
21 element drying-wetting shallow water model for rivers and estuaries. *Advances in*
22 *Water Resources*, 23, 359-372.
- 23 Horsburgh, K.J. and Wilson, C. (2007) Tide-surge interaction and its role in the distribution
24 of surge residuals in the North Sea. *Journal of Geophysical Research*, 112, C08003,
25 doi:10.1029/2006JC004033.

- 1 Ip, J.T.C., Lynch, D.R. and Friedrichs, C.T. (1998) Simulation of estuarine flooding and
2 dewatering with application to Great Bay, New Hampshire. *Estuarine Coastal and*
3 *Shelf Science*, 47, 119-141.
- 4 Jones, J.E. (2002) Coastal and shelf-sea modelling in the European context. *Oceanography*
5 *and Marine Biology: an Annual Review*, 40, 37-141.
- 6 Jones, J.E. and Davies, A.M. (1998) Storm surge computations for the Irish Sea using a
7 three-dimensional numerical model including wave-current interaction. *Continental*
8 *Shelf Research*, 18, 201-251.
- 9 Jones, J.E. and Davies, A.M. (2001) Influence of wave-current interaction and high
10 frequency forcing upon storm induced currents and elevations. *Estuarine Coastal and*
11 *Shelf Science*, 53, 397-414.
- 12 Jones, J.E. and Davies, A.M. (2003a) Processes influencing storm-induced currents in the
13 Irish Sea. *Journal of Physical Oceanography*, 33, 88-104.
- 14 Jones, J.E. and Davies, A.M. (2003b) On combining current observations and models to
15 investigate the wind induced circulation of the eastern Irish Sea. *Continental Shelf*
16 *Research*, 23, 415-434.
- 17 Jones, J.E. and Davies, A.M. (2005) An intercomparison between finite difference and finite
18 element (TELEMAC) approaches to modelling west coast of Britain tides. *Ocean*
19 *Dynamics*, 55, 178-198.
- 20 Jones, J.E. and Davies, A.M. (2006) On the sensitivity of tidal residuals off the west coast of
21 Britain to mesh resolution. *Continental Shelf Research* , 27, 64-81.
- 22 Jones, J.E. and Davies, A.M. (2007a) Influence of non-linear effects upon surge elevations
23 along the west coast of Britain (under review).
- 24 Jones, J.E. and Davies, A.M. (2007b) On the sensitivity of computed higher tidal harmonics
25 to mesh size in a finite element model *Continental Shelf Research* , 27, 1908-1927.

- 1 Legrand, S. Deleersnijder, E., Hanert, E., Legat, V. and Wolanski, E. (2006) High-resolution,
2 unstructured meshes for hydrodynamic models of the Great Barrier Reef, Australia.
3 Estuarine, Coastal and Shelf Science, 68, 36-46.
- 4 Legrand, S. Deleersnijder, E., Delhez, E. and Legat, V. (2007) Unstructured, anisotropic
5 mesh generation for the Northwestern European continental shelf, the continental
6 slope and the neighbouring ocean. Continental Shelf Research (in press).
- 7 Lennon, G.W. (1963) The identification of weather conditions associated with the generation
8 of major storm surges along the west coast of the British Isles. Quarterly Journal of
9 the Royal Meteorological Society, 89, 381-394.
- 10 Levasseur, A., Shi, L., Wells, N.C., Purdie, D.A. and Kelly-Gerreyn, B.A. (2007) A three-
11 dimensional hydrodynamic model of estuarine circulation with an application to
12 Southampton Water, U.K. Estuarine Coastal and Shelf Science.
- 13 Nicolle, A. and Karpytchev, M. (2007) Evidence for spatially variable friction from tidal
14 amplification and asymmetry in a shallow semi-diurnal embayment: the Pertuis
15 Breton Bay of Biscay, France. Continental Shelf Research.
- 16 Prandle, D. and Wolf, J. (1978) The interaction of surge and tide in the North Sea and River
17 Thames. Geophysical Journal of the Royal Astronomical Society, 55, 203-216.
- 18 Walters, R.A. (2005) Coastal ocean models: two useful finite element methods. Continental
19 Shelf Research, 25, 775-793.
- 20 Werner, F.E. (1995) A field test case for tidally forced flows: a review of the tidal flow
21 forum pg. 269-284 in Quantitative Skill Assessment for Coastal Ocean Models, ed.
22 D.R. Lynch and A.M. Davies, published American Geophysical Union.
- 23

1 FIGURE CAPTIONS

- 2 Fig. 1: Model domain, with open boundary denoted by dashed line, and water depths
3 (m) given by contours. Also shown are locations of place names.
- 4 Fig. 2: Expanded version of Fig. 1 in the eastern Irish Sea.
- 5 Fig. 3: The unstructured finite element grid used in the calculations.
- 6 Fig. 4: Steady state elevations (m) in the Eastern Irish Sea due to a uniform west
7 wind of 1.0 Pa applied over the model domain.
- 8 Fig. 5: An enlargement of the Morecambe Bay region of Fig. 4
- 9 Fig. 6: Contours (cm) of the change in amplitude of (a) M_2 , (b) M_4 and (c) M_6
10 components of the tide in Morecambe Bay due to a uniform west wind of 1.0
11 Pa.
- 12 Fig. 7: As Fig. 6, but in Liverpool Bay.
- 13 Fig. 8: Steady state elevations (m) in the Eastern Irish Sea due to a
14 uniform north wind of 1.0 Pa applied over the model domain.
- 15 Fig. 9: An enlargement of the Morecambe Bay region of Fig. 8.
- 16 Fig. 10: Steady state Elevations (m) in the Eastern Irish Sea due to a uniform
17 south wind of 1.0 Pa
- 18 Fig. 11: Contours (cm) of the change in amplitude of (a) M_2 , (b) M_4 and (c) M_6
19 in Morecambe Bay due to a uniform north wind of 1.0 Pa.
- 20 Fig. 12: Contours (cm) of the change in amplitude of (a) M_2 , (b) M_4 and (c) M_6 in
21 Liverpool Bay due to a uniform north wind of 1.0 Pa.
- 22 Fig. 13: Contours (cm) of the change in amplitude of (a) M_2 , (b) M_4 and (c) M_6 in
23 Morecambe Bay due to a uniform south wind of 1.0 Pa..
- 24 Fig. 14: Contours (cm) of the change in amplitude of (a) M_2 , (b) M_4 and (c) M_6 in
25 Liverpool Bay due to a uniform south wind of 1.0 Pa.

- 1 Fig. 15: Change in M_2 tidal current ellipse in eastern Irish Sea due to a uniform west
2 wind of 1.0 Pa.
- 3 Fig. 16: Change in M_4 tidal current ellipse in eastern Irish Sea due to a uniform west
4 wind of 1.0 Pa.
- 5 Fig. 17: Change in M_6 tidal current ellipse in eastern Irish Sea due to a uniform west
6 wind of 1.0 Pa.
- 7 Fig. 18: Change in (a) M_2 , (b) M_4 , and (c) M_6 tidal current ellipses in Morecambe Bay
8 due to a uniform west wind of 1.0 Pa.
- 9 Fig. 19: Change in (a) M_2 , (b) M_4 , and (c) M_6 tidal current ellipses in Liverpool Bay
10 due to a uniform west wind of 1.0 Pa.
- 11 Fig. 20: Time series over the last two tidal cycles at location A, of (a) free surface
12 elevation in the absence of wind (solid line), (b) free surface elevation with
13 a south wind of 1.0 Pa (dashed line), (c) free surface elevation with a north
14 wind of 1.0 Pa (dotted line).
- 15 Fig. 21: Change in two components of bottom friction ($\text{m s}^{-2} \times 10^6$) at location A,
16 due to (a) a south wind of 1.0 Pa (dashed line), and (b) a north wind of
17 1.0 Pa (dotted line). (Note scaled by 10^6).
- 18 Fig. 22: Change in momentum advection terms ($\text{m s}^{-2} \times 10^6$) udu/dx , vdu/dy ,
19 udv/dx and vdv/dy at location A, due to (a) a south wind of 1.0 Pa (dashed
20 line) and (b) a north wind of 1.0 Pa (dotted line). (Note: scaled by 10^6).
- 21 Fig. 23: As Fig. 20 but at location B.
- 22 Fig. 24: As Fig. 21 but at location B. (Note scaled by 10^6).
- 23 Fig. 25: As Fig. 22 but at location B. (Note, scaled by 10^6)
24

1 Table 1: Summary of Calculations

2

| Calc. | Wind Direction |
|-------|----------------|
| 1. | West |
| 2. | North |
| 3. | South |

3

4

5

1 Table 2a: Spatial variability of computed M_2 amplitude (A) and phase (g) at a number of tide
 2 gauges and influence of west (Calc 1), south (Calc 2) and north (Calc 3) wind stress of 1.0
 3 Pa.
 4

| Port | Dist from Port Δ (km) | Water Depth h (m) | Tide only | | Calc 1 tide + west wind | | Calc 2 tide + north wind | | Calc 3 tide + south wind | |
|---------------|------------------------------------|-------------------------|-----------|---------------------|-------------------------------|---------------------|--------------------------------|---------------------|--------------------------------|---------------------|
| | | | A (cm) | g ($^{\circ}$) | A (cm) | g ($^{\circ}$) | A (cm) | g ($^{\circ}$) | A (cm) | g ($^{\circ}$) |
| Hilbre | 1.1 | 9.6 | 319 | 309 | 309 | 310 | 307 | 310 | 323 | 309 |
| | 1.1 | 2.0 | 275 | 307 | 291 | 308 | 265 | 307 | 282 | 307 |
| | 1.3 | 16.2 | 324 | 307 | 314 | 308 | 313 | 308 | 327 | 307 |
| | 1.8 | 2.3 | 294 | 308 | 306 | 308 | 285 | 308 | 299 | 307 |
| | | | | | | | | | | |
| Conwy | 1.1 | 1.3 | 223 | 299 | 237 | 300 | 201 | 297 | 230 | 299 |
| | 2.1 | 0.6 | 179 | 297 | 194 | 297 | 163 | 296 | 189 | 297 |
| | 2.5 | 1.3 | 221 | 298 | 233 | 299 | 202 | 297 | 229 | 298 |
| | 3.4 | 2.0 | 257 | 298 | 263 | 298 | 245 | 298 | 262 | 298 |
| | | | | | | | | | | |
| Barrow RI | 1.0 | 0.0 | 162 | 321 | 178 | 322 | 123 | 319 | 195 | 322 |
| | 1.0 | 0.0 | 160 | 314 | 177 | 315 | 120 | 311 | 196 | 315 |
| | 1.9 | 9.1 | 321 | 323 | 321 | 323 | 319 | 326 | 307 | 322 |
| | 2.2 | 6.4 | 323 | 326 | 326 | 326 | 324 | 328 | 309 | 324 |
| | | | | | | | | | | |
| Barrow HP | 1.0 | 9.1 | 321 | 323 | 321 | 323 | 319 | 326 | 307 | 322 |
| | 1.1 | 5.9 | 319 | 323 | 319 | 323 | 322 | 325 | 307 | 321 |
| | 1.6 | 3.3 | 320 | 326 | 321 | 326 | 308 | 327 | 310 | 325 |
| | 2.1 | 0.0 | 162 | 321 | 178 | 322 | 124 | 319 | 195 | 322 |
| | | | | | | | | | | |
| Liverpool P.P | 0.18 | 8.2 | 321 | 313 | 307 | 313 | 314 | 314 | 319 | 312 |
| | | | | | | | | | | |
| Liverpool Bay | 0.57 | 11.2 | 317 | 306 | 311 | 306 | 313 | 306 | 313 | 305 |
| | | | | | | | | | | |
| SN 35 | 1.59 | 33.3 | 276 | 319 | 272 | 320 | 273 | 319 | 269 | 319 |

5
 6
 7

1 Table 2b: Spatial variability of computed M_4 amplitude (A) and phase (g) at a number of tide
 2 gauges and influence of west (Calc 1), south (Calc 2) and north (Calc 3) wind stress of 1.0
 3 Pa.
 4

| Port | Dist from Port Δ (km) | Water Depth h (m) | Tide only | | Calc 1 tide + west wind | | Calc 2 tide + north wind | | Calc 3 tide + south wind | |
|---------------|------------------------------------|-------------------------|-----------|---------------------|-------------------------------|---------------------|--------------------------------|---------------------|--------------------------------|---------------------|
| | | | A (cm) | g ($^{\circ}$) | A (cm) | g ($^{\circ}$) | A (cm) | g ($^{\circ}$) | A (cm) | g ($^{\circ}$) |
| Hilbre | 1.1 | 9.6 | 27.6 | 158 | 29.6 | 168 | 33.3 | 178 | 24.3 | 137 |
| | 1.1 | 2.0 | 32.8 | 227 | 26.0 | 201 | 40.3 | 229 | 23.6 | 224 |
| | 1.3 | 16.2 | 28.2 | 152 | 28.7 | 164 | 33.5 | 172 | 24.5 | 131 |
| | 1.8 | 2.3 | 28.8 | 210 | 27.4 | 181 | 36.0 | 213 | 19.0 | 203 |
| Conwy | 1.1 | 1.3 | 39.7 | 223 | 31.3 | 215 | 45.7 | 228 | 33.4 | 224 |
| | 2.1 | 0.6 | 53.6 | 232 | 46.2 | 232 | 58.6 | 229 | 46.7 | 232 |
| | 2.5 | 1.3 | 40.0 | 227 | 31.4 | 223 | 49.4 | 229 | 31.4 | 229 |
| | 3.4 | 2.0 | 20.3 | 214 | 13.5 | 199 | 28.5 | 213 | 10.2 | 210 |
| Barrow RI | 1.0 | 0.0 | 69.1 | 283 | 75.2 | 282 | 65.1 | 282 | 59.6 | 283 |
| | 1.0 | 0.0 | 66.0 | 275 | 70.3 | 276 | 60.7 | 270 | 54.4 | 279 |
| | 1.9 | 9.1 | 30.4 | 201 | 30.5 | 210 | 47.8 | 227 | 20.3 | 173 |
| | 2.2 | 6.4 | 32.1 | 204 | 32.0 | 213 | 48.3 | 228 | 22.4 | 176 |
| Barrow HP | 1.0 | 9.1 | 30.4 | 201 | 30.5 | 210 | 47.8 | 227 | 20.3 | 173 |
| | 1.1 | 5.9 | 28.3 | 203 | 28.8 | 214 | 44.6 | 222 | 16.7 | 178 |
| | 1.6 | 3.3 | 25.0 | 209 | 26.6 | 221 | 36.2 | 241 | 15.2 | 182 |
| | 2.1 | 0.0 | 69.1 | 283 | 75.2 | 282 | 65.1 | 282 | 59.6 | 283 |
| Liverpool P.P | 0.18 | 8.2 | 30.8 | 148 | 24.7 | 155 | 35.6 | 167 | 27.7 | 128 |
| Liverpool Bay | 0.57 | 11.2 | 20.4 | 145 | 20.7 | 157 | 26.0 | 164 | 17.3 | 119 |
| SN 35 | 1.59 | 33.3 | 11.9 | 162 | 9.2 | 185 | 12.0 | 203 | 14.6 | 137 |

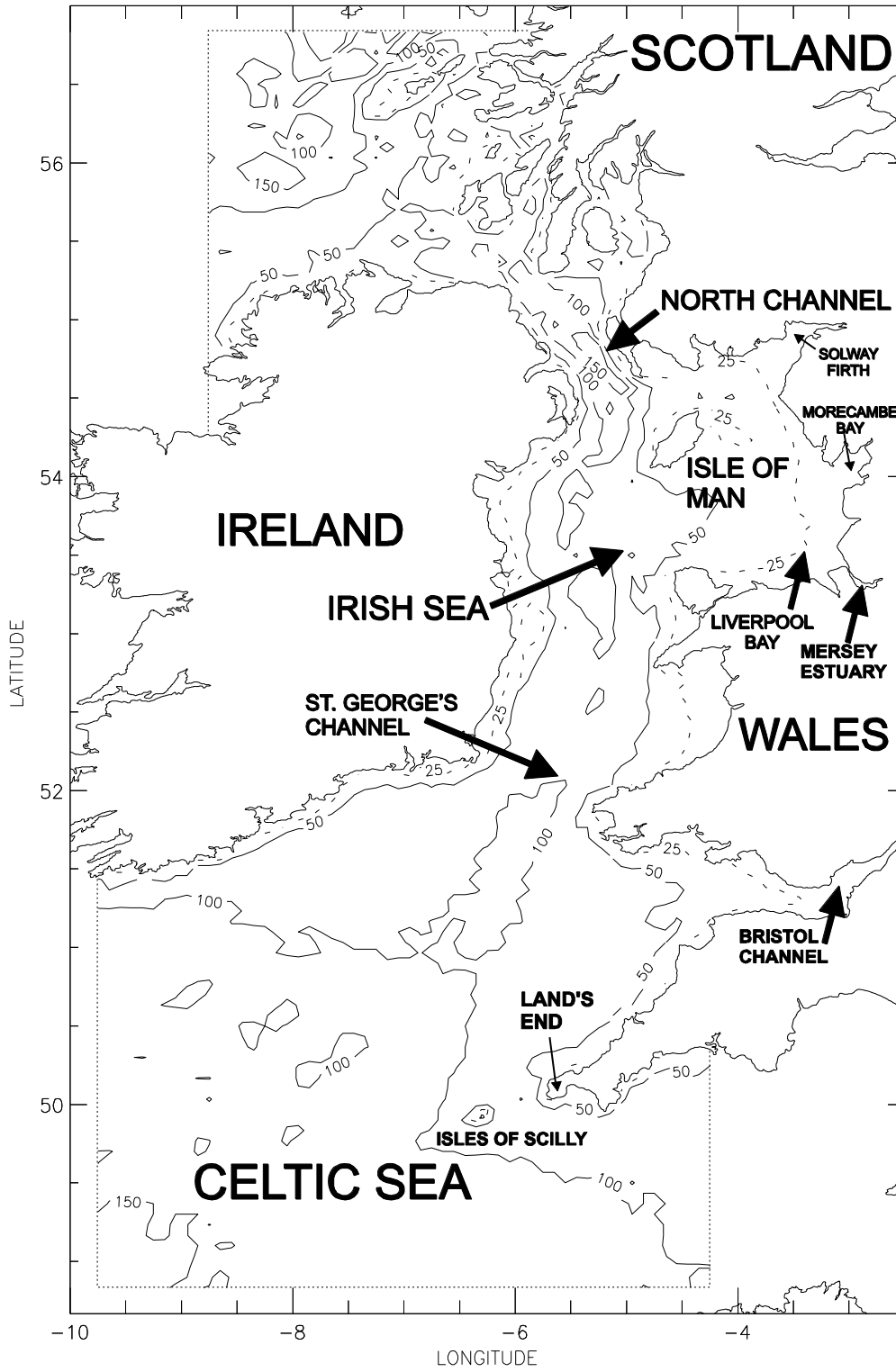
5
6
7

1 Table 2c: Spatial variability of computed M_6 amplitude (A) and phase (g) at a number of tide
 2 gauges and influence of west (Calc 1), south (Calc 2) and north (Calc 3) wind stress of 1.0
 3 Pa.
 4

| Port | Dist from Port Δ (km) | Water Depth h (m) | Tide only | | Calc 1 tide + west wind | | Calc 2 tide + north wind | | Calc 3 tide + south wind | |
|---------------|------------------------------------|-------------------------|-----------|---------------------|-------------------------------|---------------------|--------------------------------|---------------------|--------------------------------|---------------------|
| | | | A (cm) | g ($^{\circ}$) | A (cm) | g ($^{\circ}$) | A (cm) | g ($^{\circ}$) | A (cm) | g ($^{\circ}$) |
| Hilbre | 1.1 | 9.6 | 6.8 | 328 | 7.8 | 311 | 6.9 | 340 | 8.1 | 321 |
| | 1.1 | 2.0 | 23.4 | 32 | 12.2 | 28 | 21.1 | 40 | 23.9 | 22 |
| | 1.3 | 16.2 | 7.9 | 316 | 8.2 | 307 | 7.5 | 327 | 9.3 | 306 |
| | 1.8 | 2.3 | 21.7 | 28 | 9.2 | 354 | 20.2 | 35 | 20.6 | 17 |
| Conwy | 1.1 | 1.3 | 22.5 | 10 | 22.5 | 7 | 18.4 | 27 | 24.4 | 4 |
| | 2.1 | 0.6 | 14.2 | 3 | 16.9 | 4 | 8.2 | 16 | 18.5 | 354 |
| | 2.5 | 1.3 | 22.6 | 7 | 20.0 | 7 | 21.6 | 19 | 23.3 | 1 |
| | 3.4 | 2.0 | 16.9 | 1 | 10.1 | 359 | 17.9 | 7 | 14.1 | 348 |
| Barrow RI | 1.0 | 0.0 | 4.5 | 175 | 4.3 | 161 | 18.7 | 236 | 11.5 | 69 |
| | 1.0 | 0.0 | 5.6 | 251 | 3.7 | 248 | 18.4 | 238 | 10.2 | 38 |
| | 1.9 | 9.1 | 11.7 | 9 | 7.7 | 344 | 19.4 | 61 | 14.2 | 306 |
| | 2.2 | 6.4 | 11.2 | 16 | 6.7 | 348 | 17.7 | 72 | 14.5 | 307 |
| Barrow HP | 1.0 | 9.1 | 11.7 | 9 | 7.7 | 344 | 19.4 | 61 | 14.2 | 306 |
| | 1.1 | 5.9 | 13.7 | 357 | 9.7 | 337 | 15.5 | 37 | 13.2 | 307 |
| | 1.6 | 3.3 | 10.1 | 351 | 8.0 | 317 | 12.6 | 81 | 13.3 | 301 |
| | 2.1 | 0.0 | 4.5 | 175 | 4.3 | 161 | 18.7 | 236 | 11.5 | 69 |
| Liverpool P.P | 0.18 | 8.2 | 14.7 | 326 | 14.6 | 326 | 15.2 | 339 | 15.1 | 320 |
| Liverpool Bay | 0.57 | 11.2 | 5.8 | 315 | 6.4 | 308 | 5.3 | 316 | 6.8 | 306 |
| SN 35 | 1.59 | 33.3 | 1.5 | 99 | 2.7 | 89 | 2.9 | 137 | 2.3 | 17 |

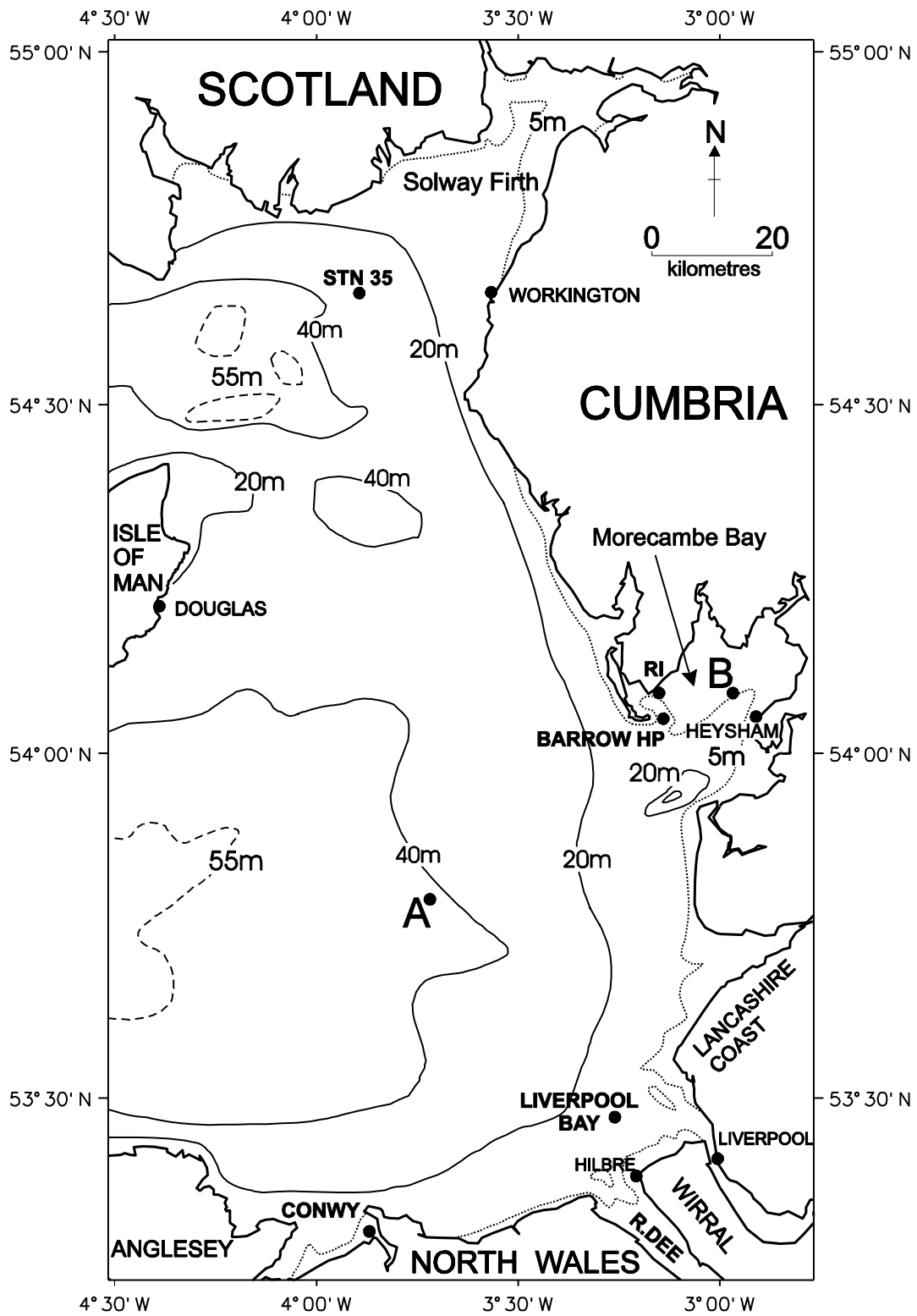
5
6
7
8
9

1 FIG 1



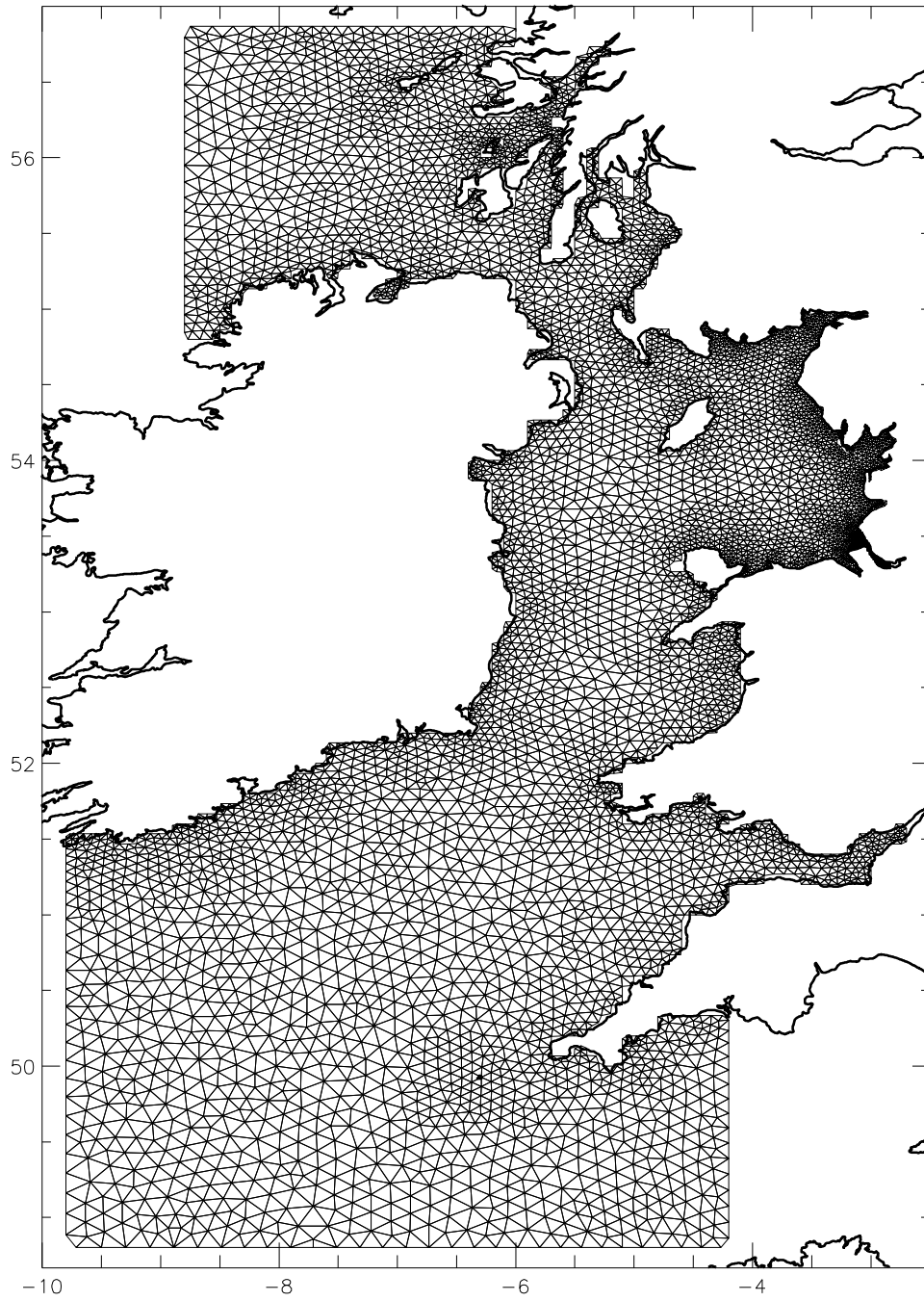
2
3
4

1 FIG 2



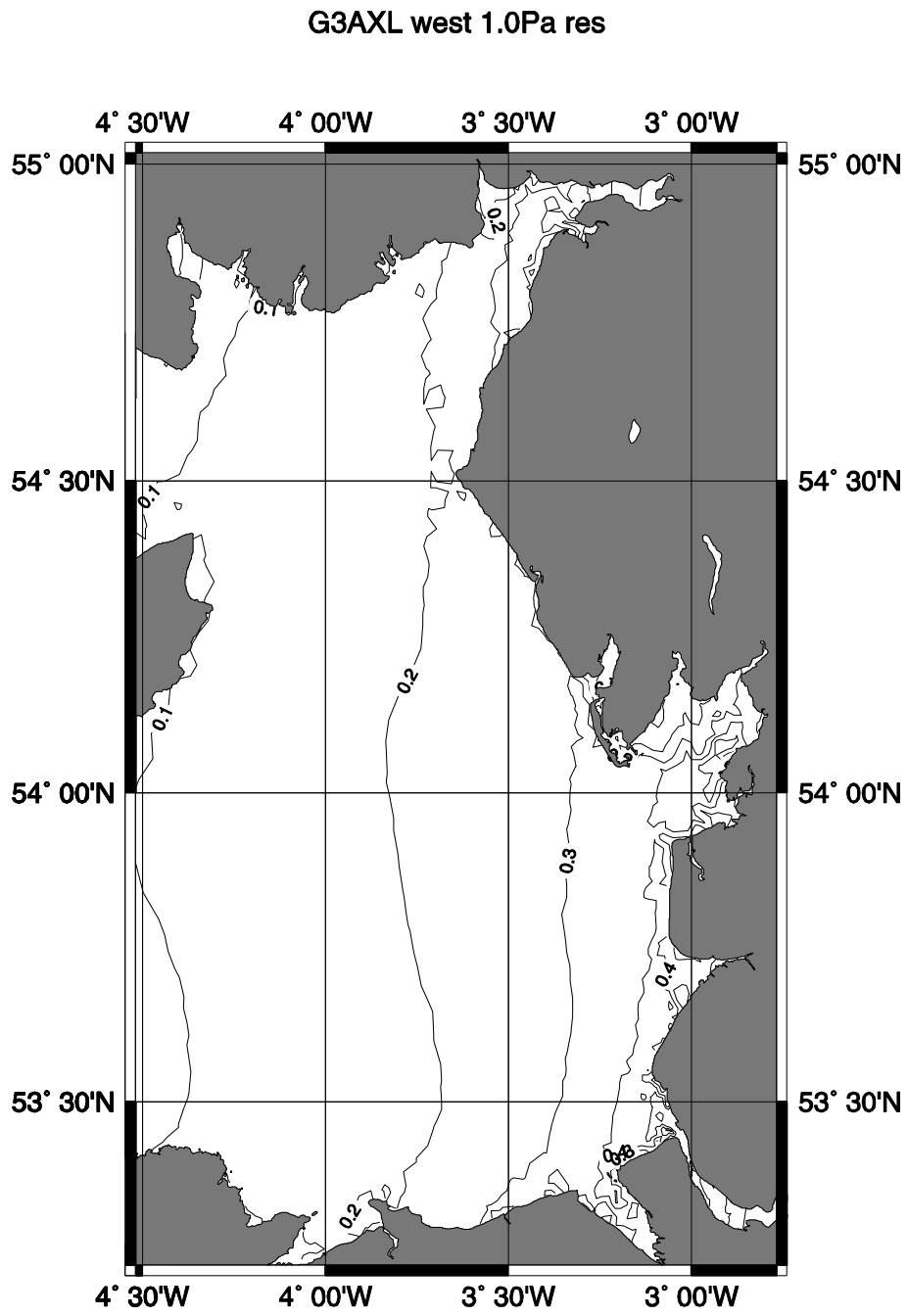
2
3
4

GRID G3AX



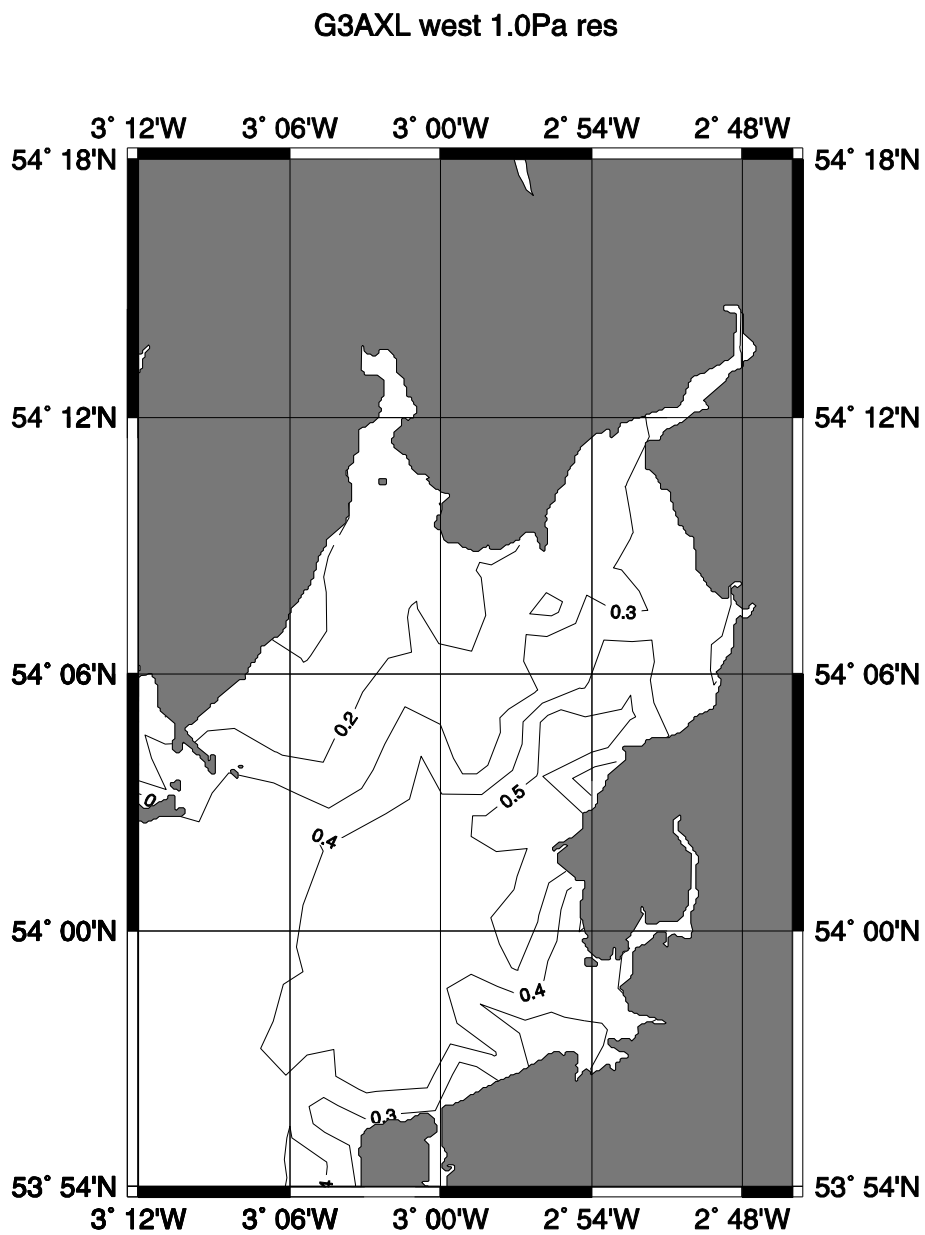
2
3
4

1 FIG 4



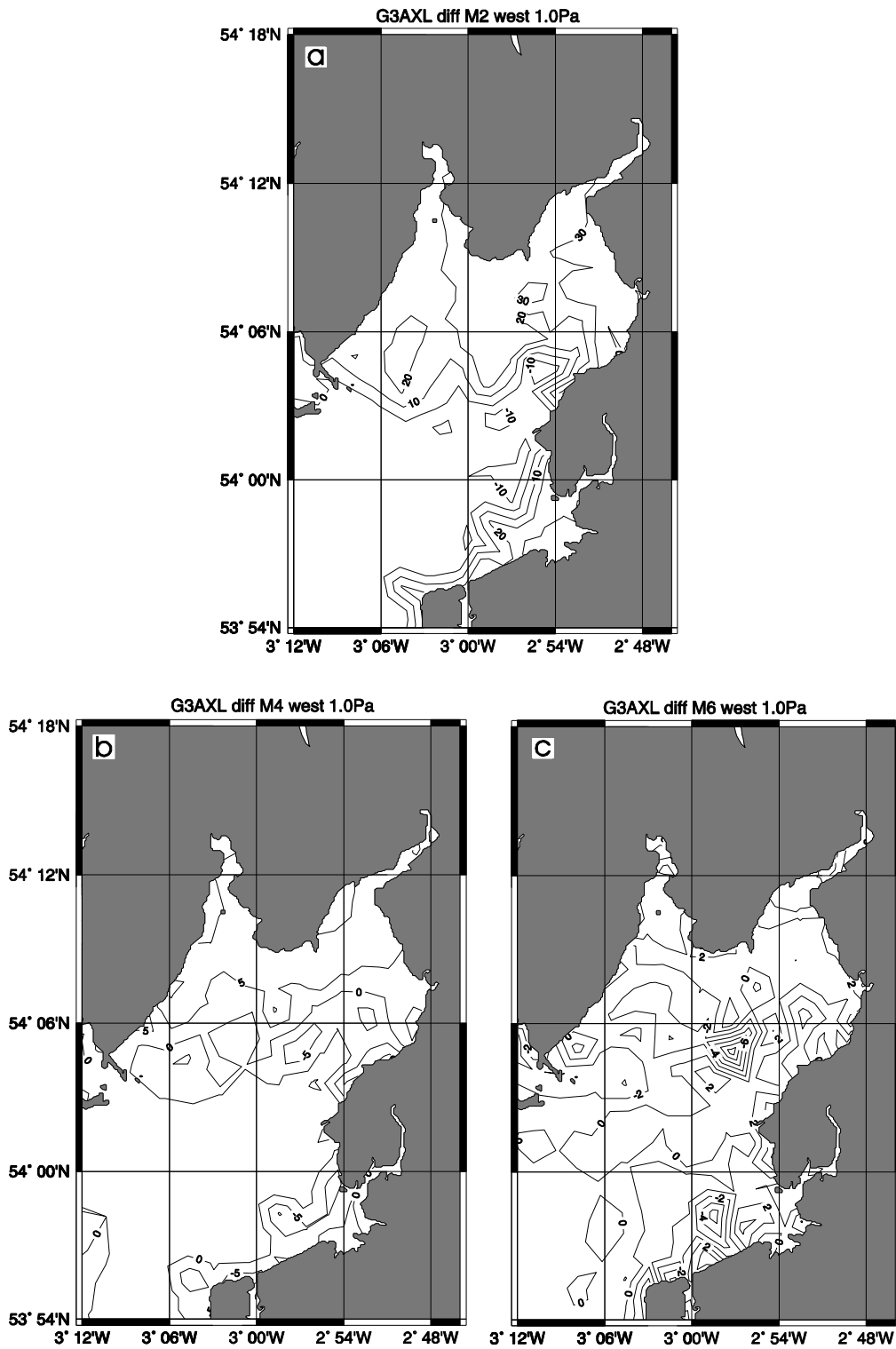
2
3
4

1 FIG 5



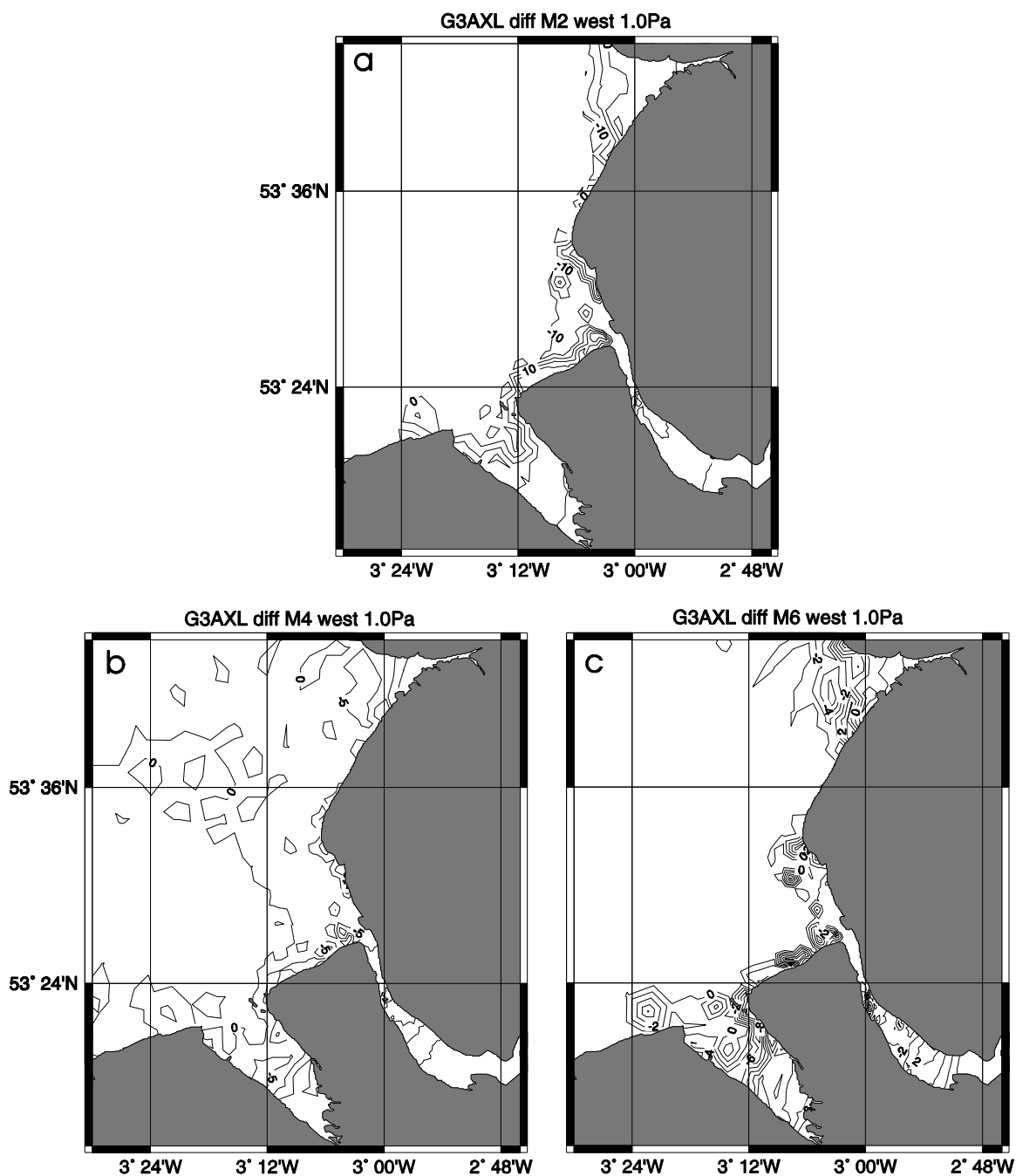
2
3
4

1 FIG 6



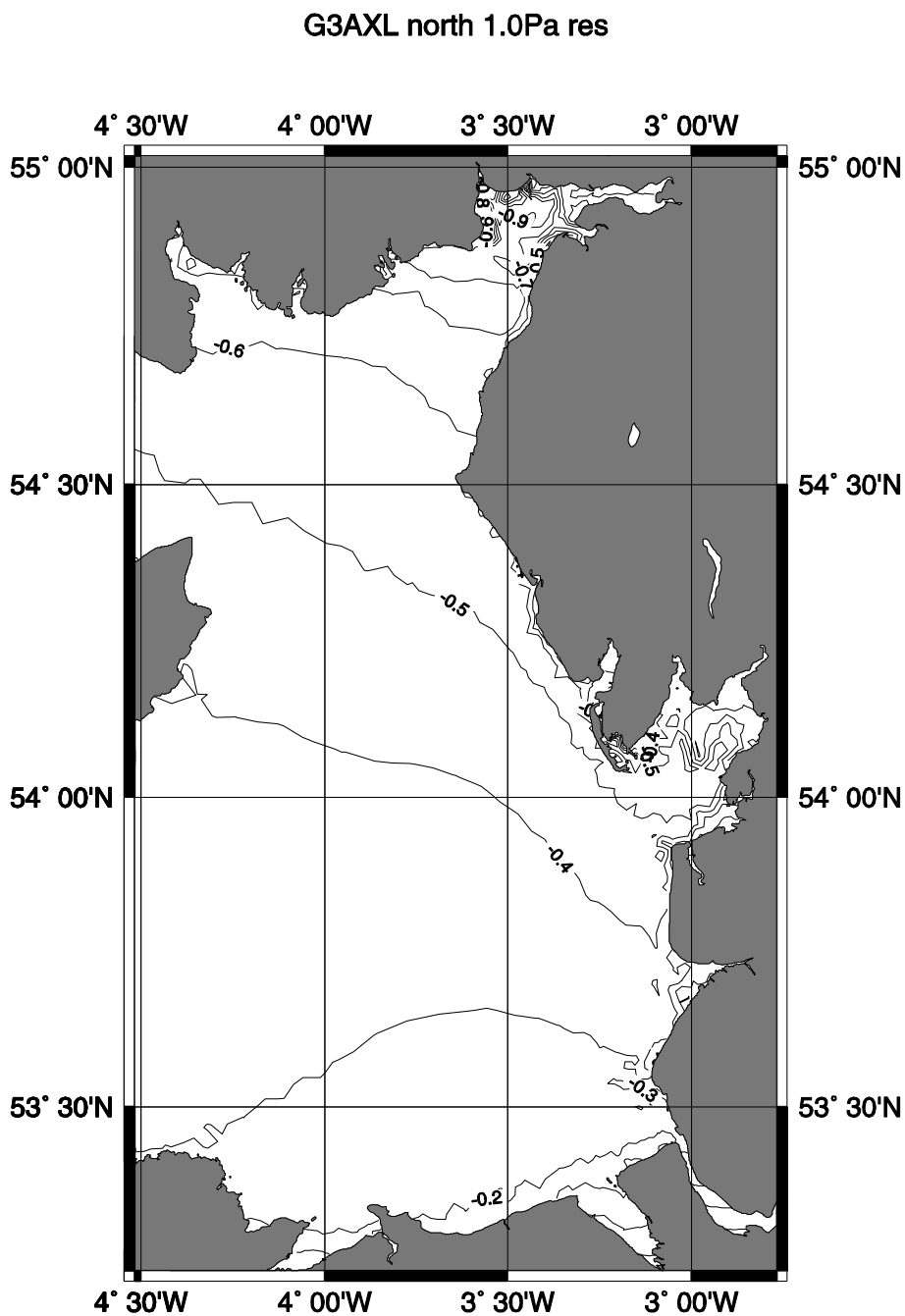
2
3
4

1 FIG 7



2
3
4

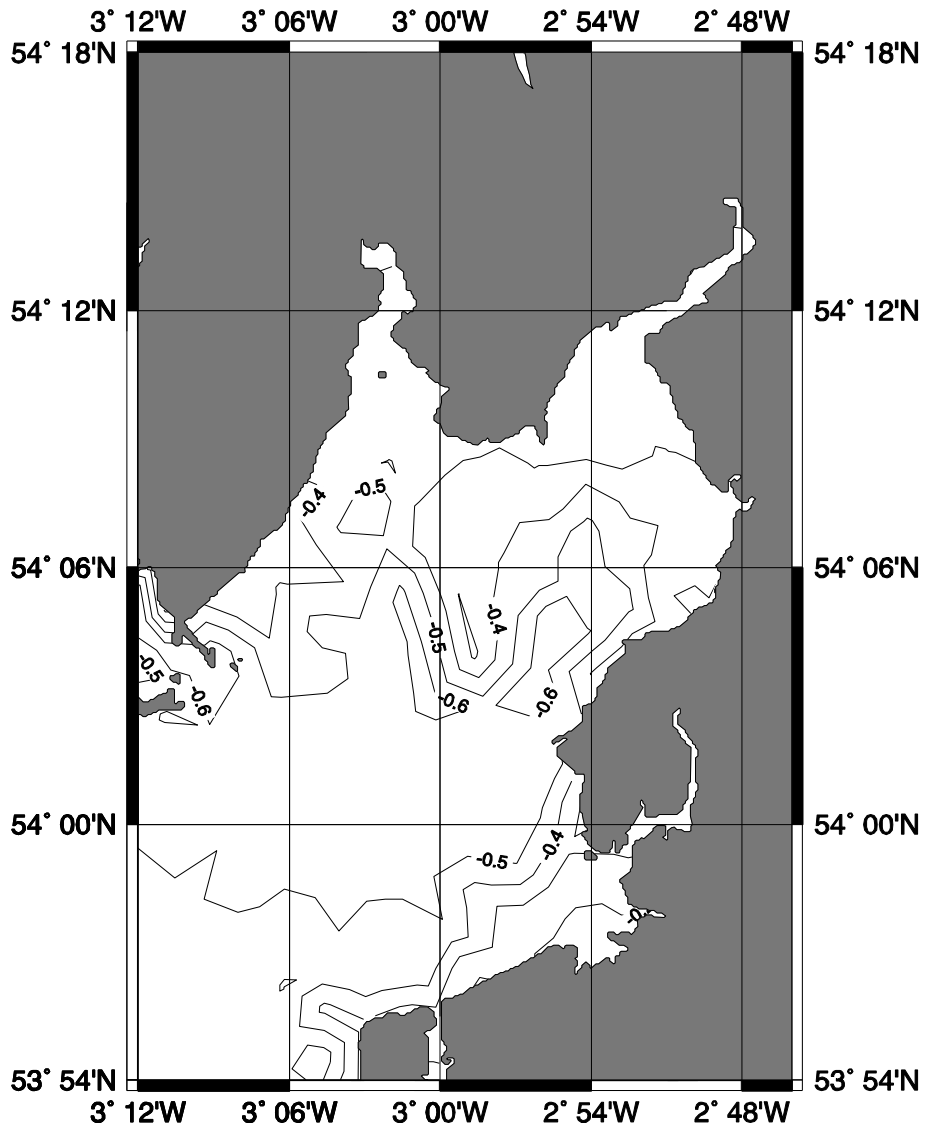
1 FIG 8



2
3
4

1 FIG 9

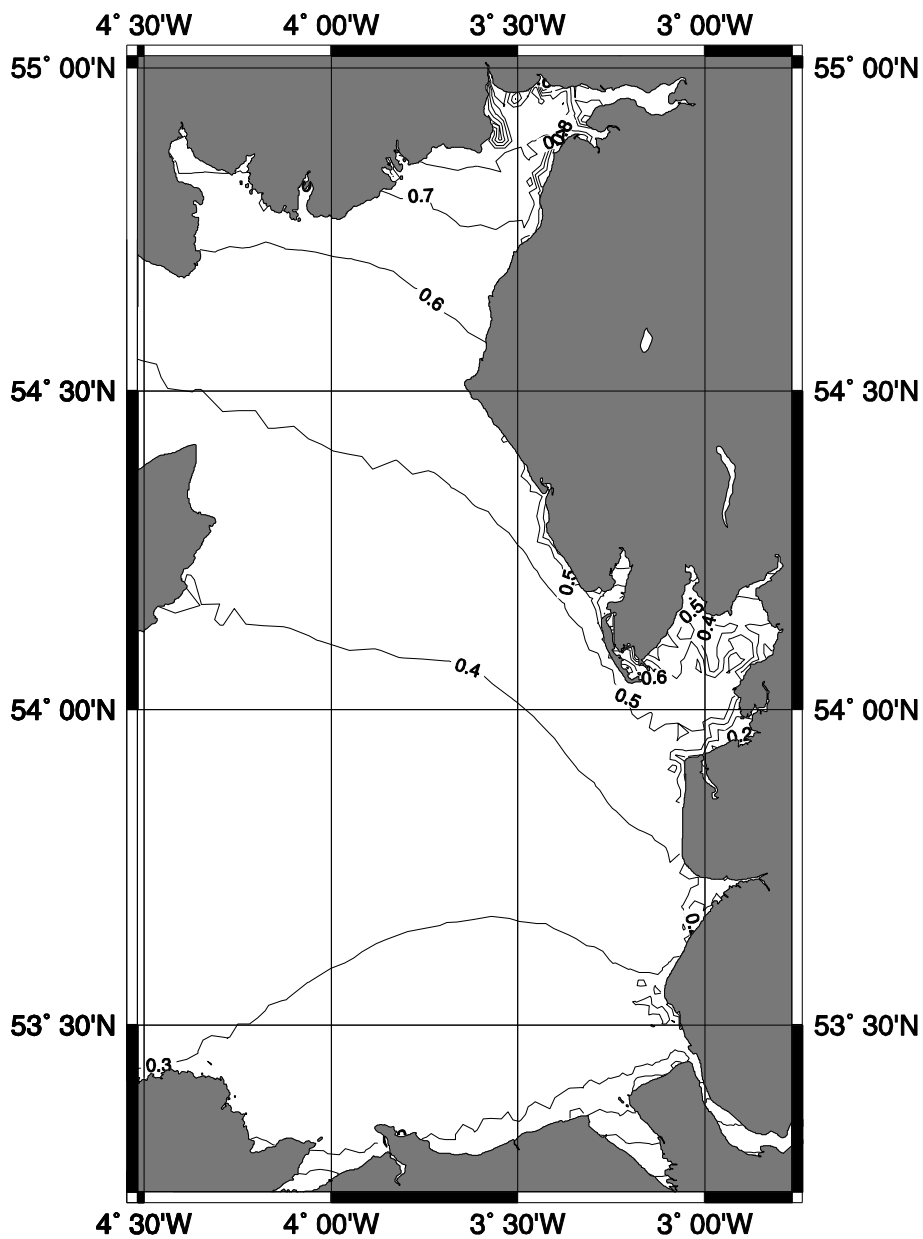
G3AXL north 1.0Pa res



- 2
- 3
- 4
- 5

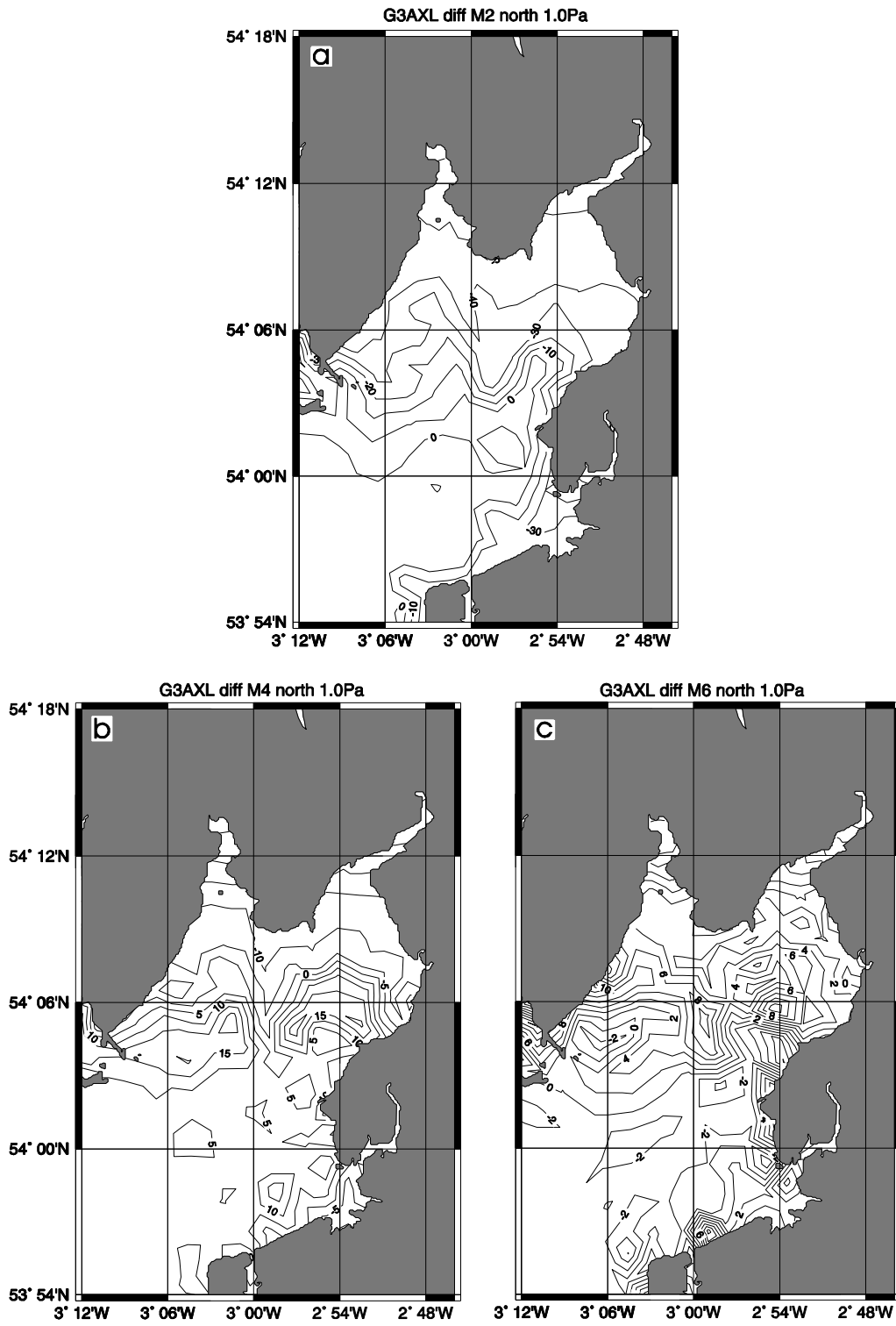
1 FIG 10

G3AXL south 1.0Pa res



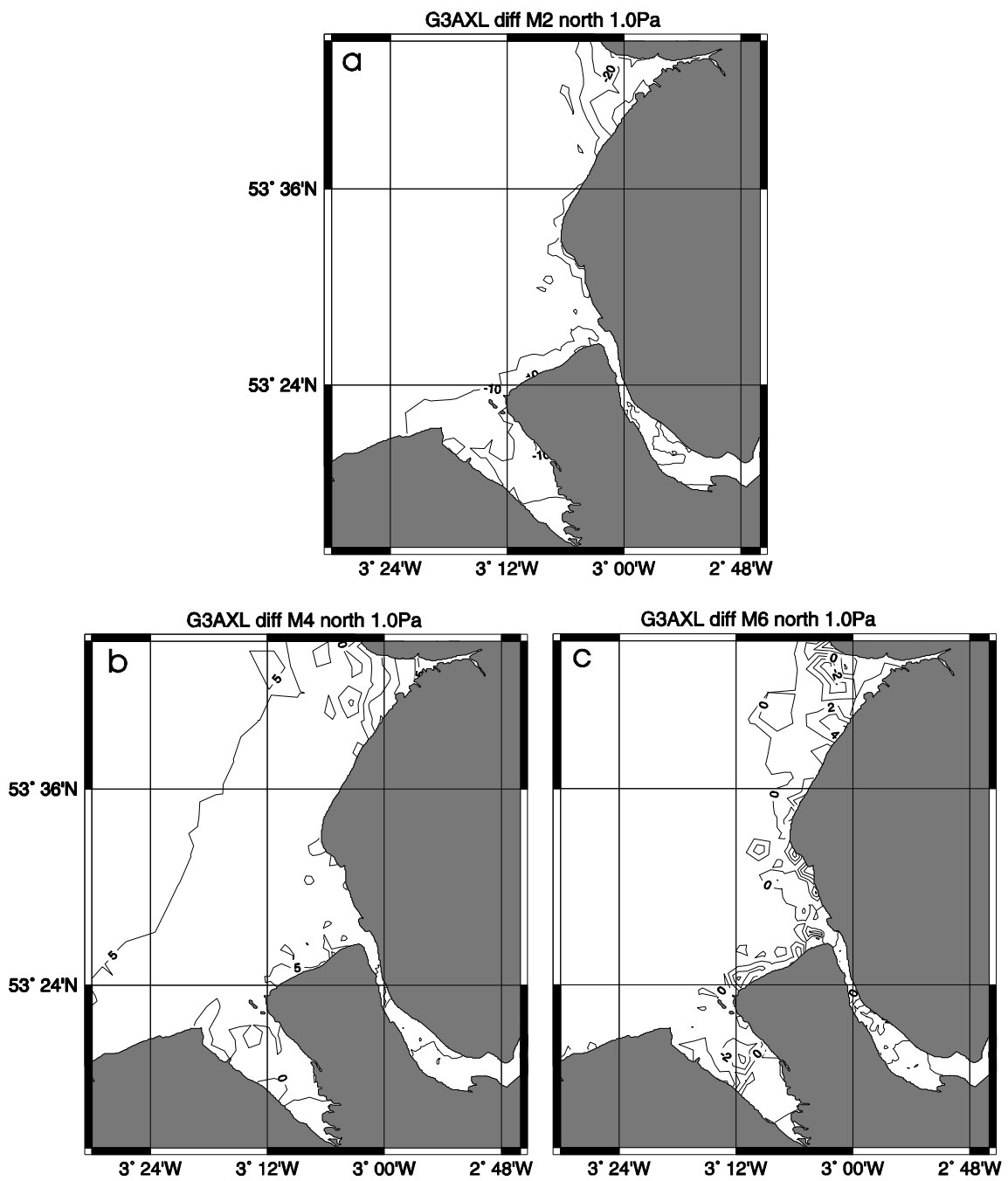
2
3
4

1 FIG 11



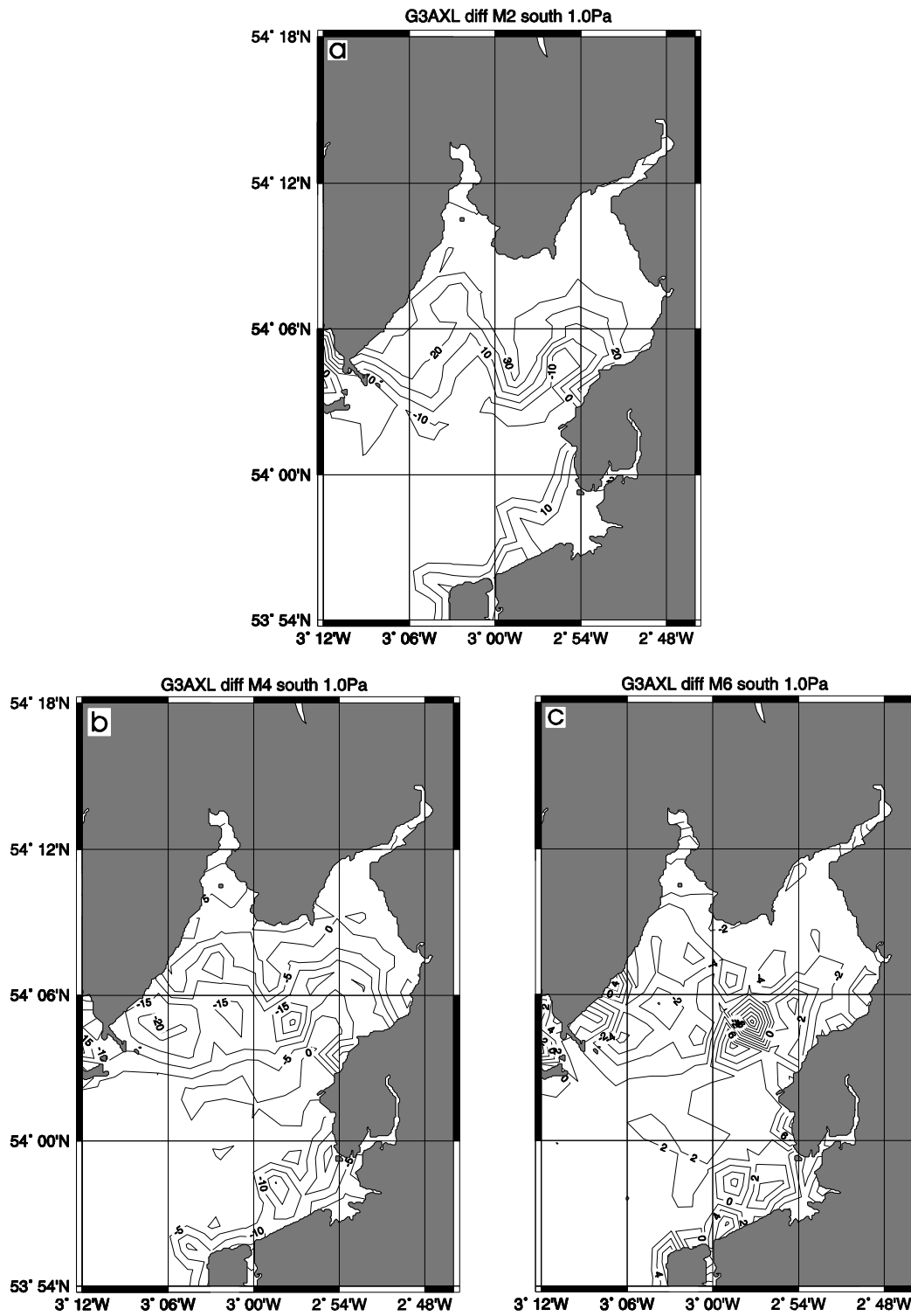
2
3
4

1 FIG 12



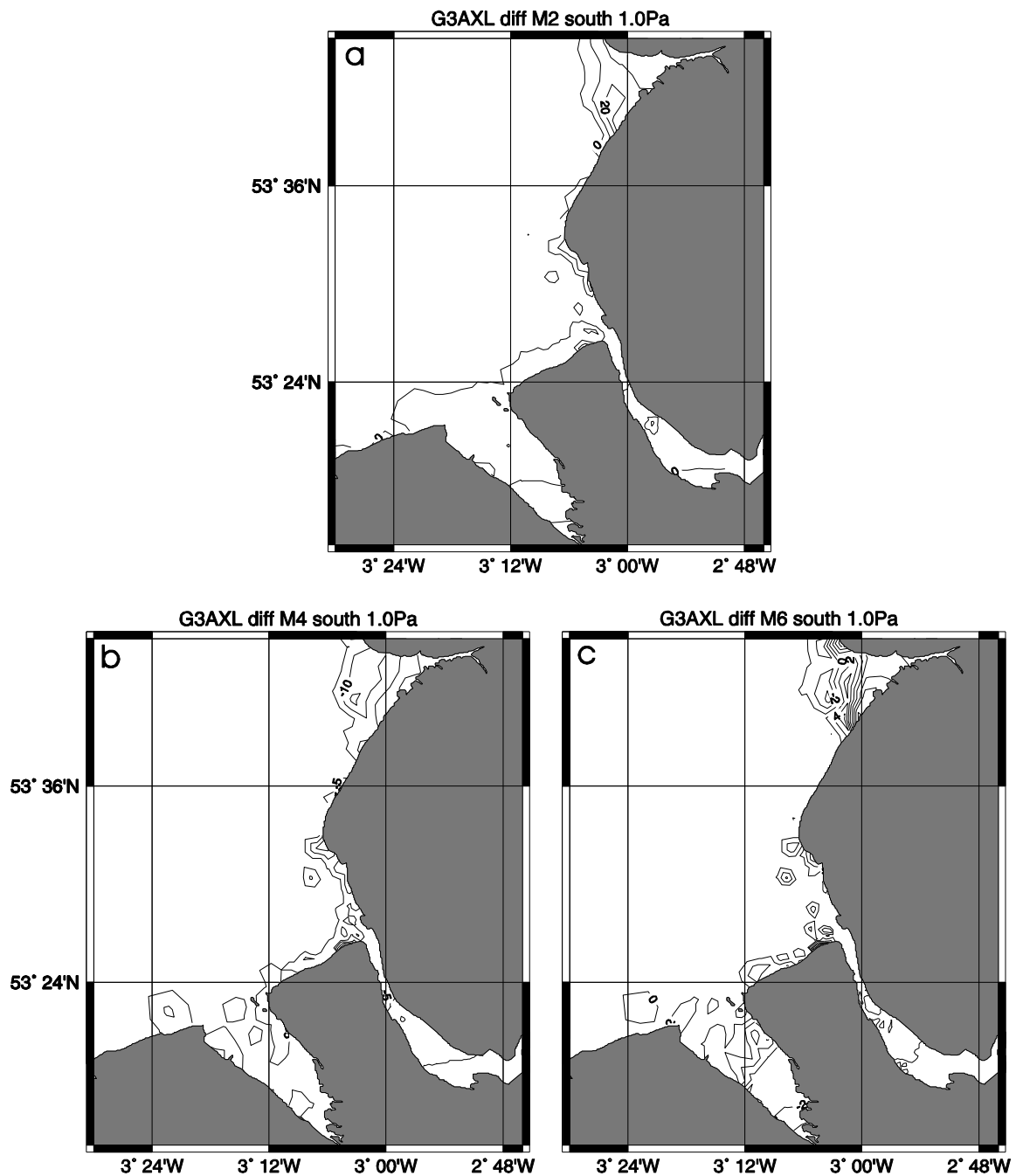
2
3
4

1 FIG 13



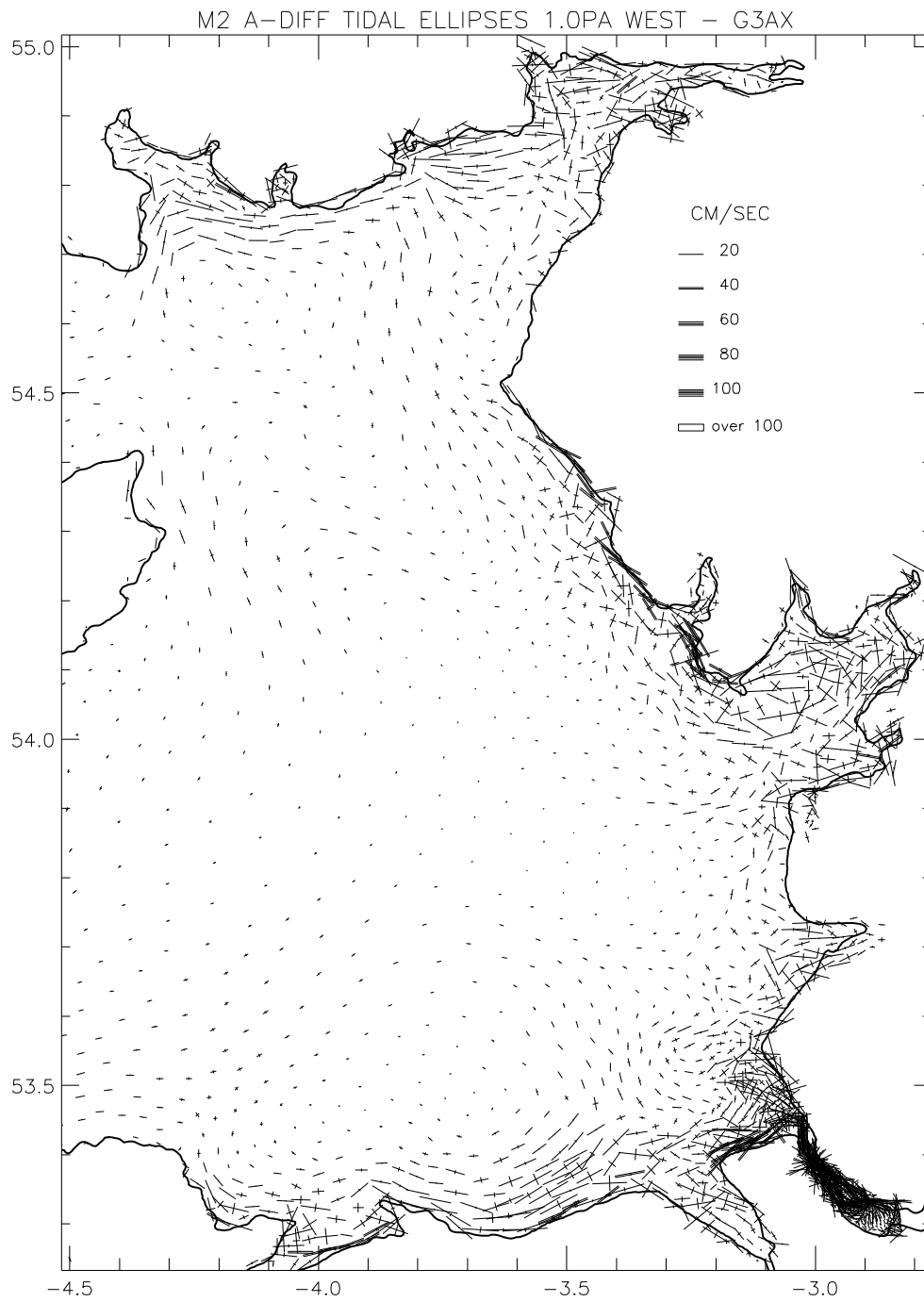
2
3
4

1 FIG 14



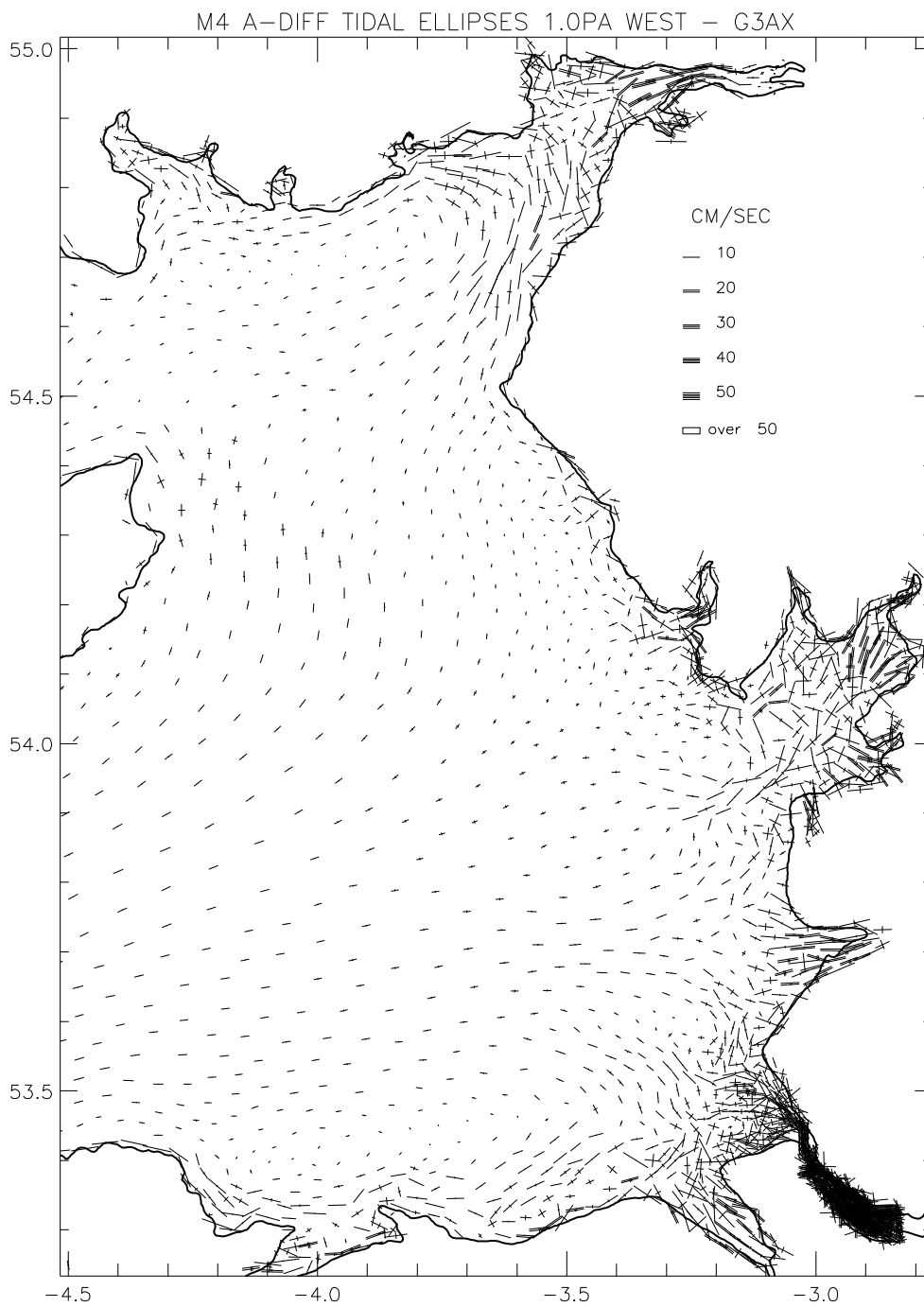
2
3
4

1 FIG 15



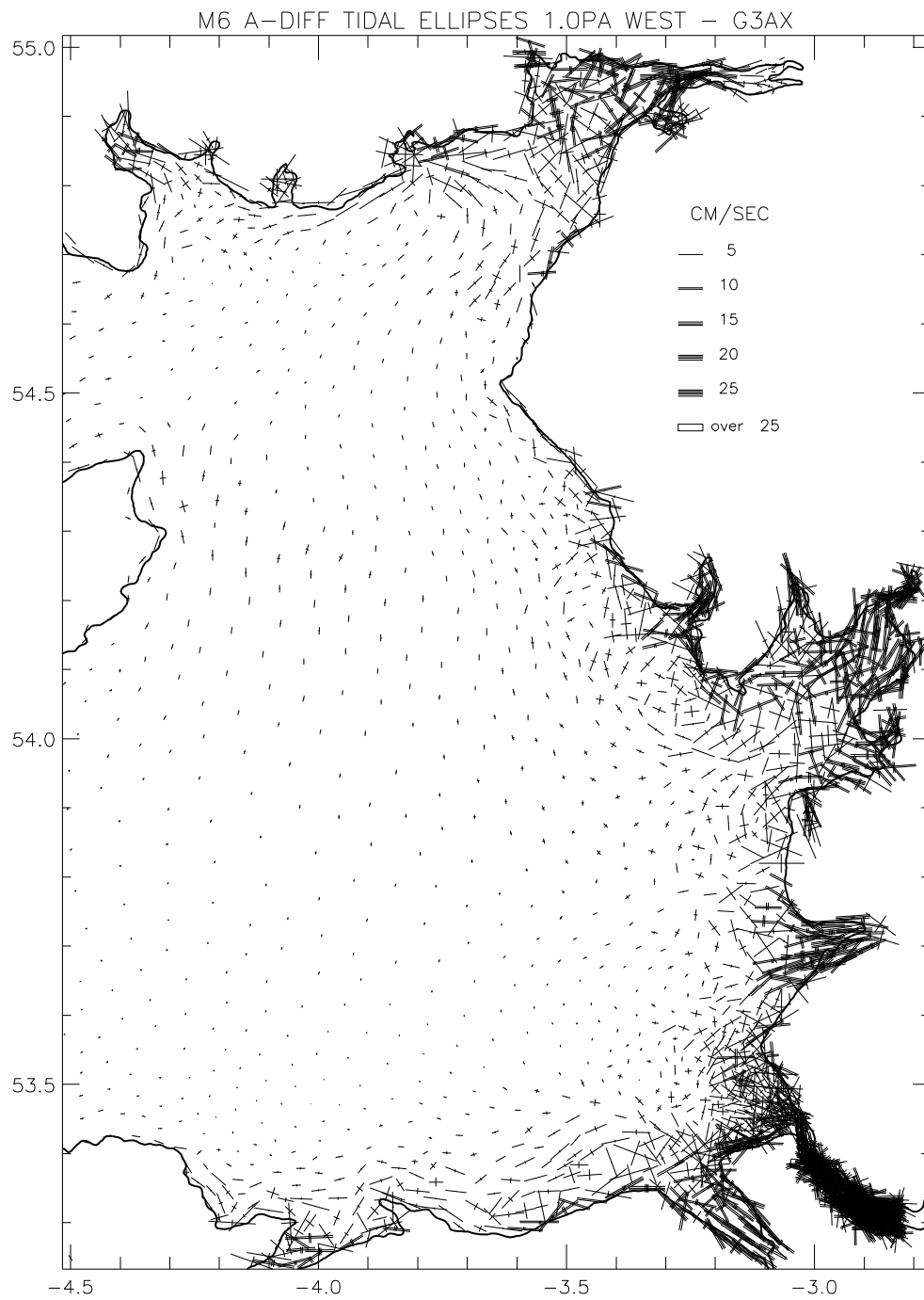
2
3
4

1 FIG 16

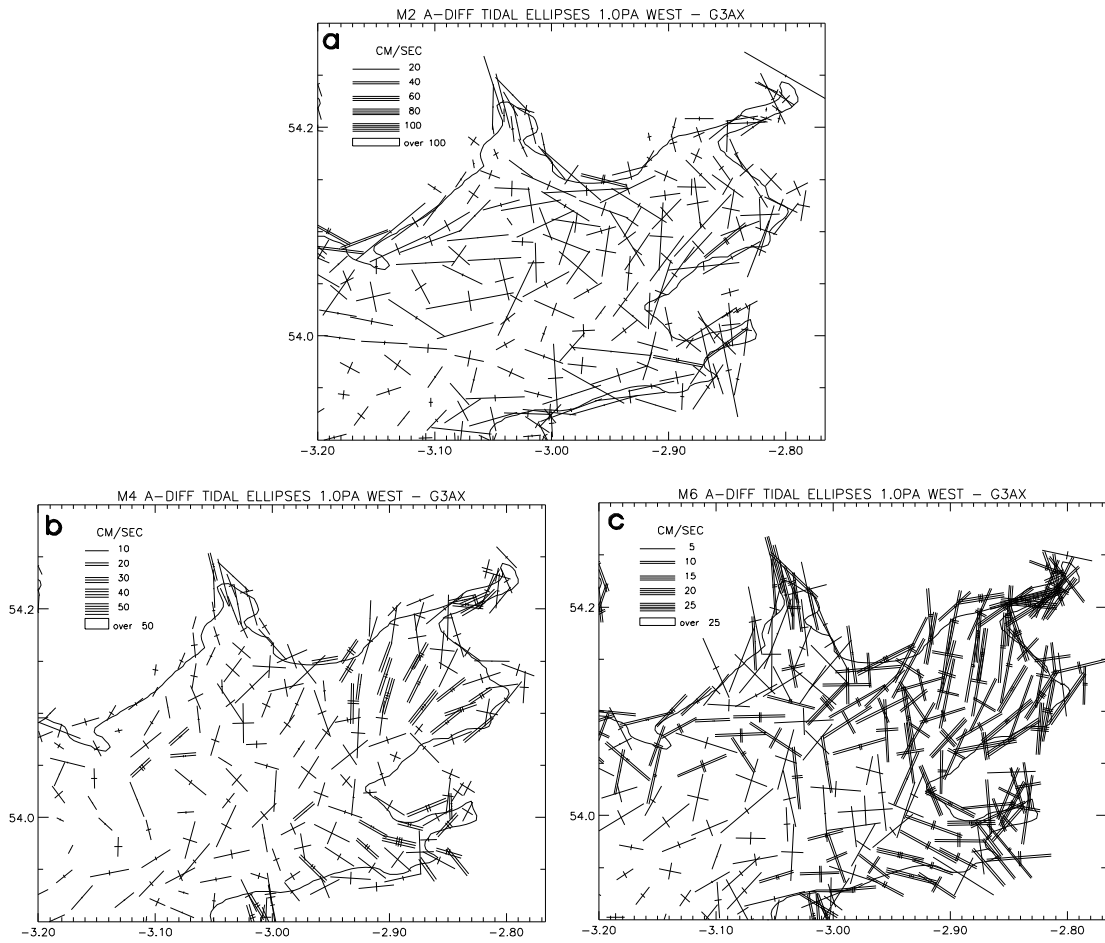


2
3
4

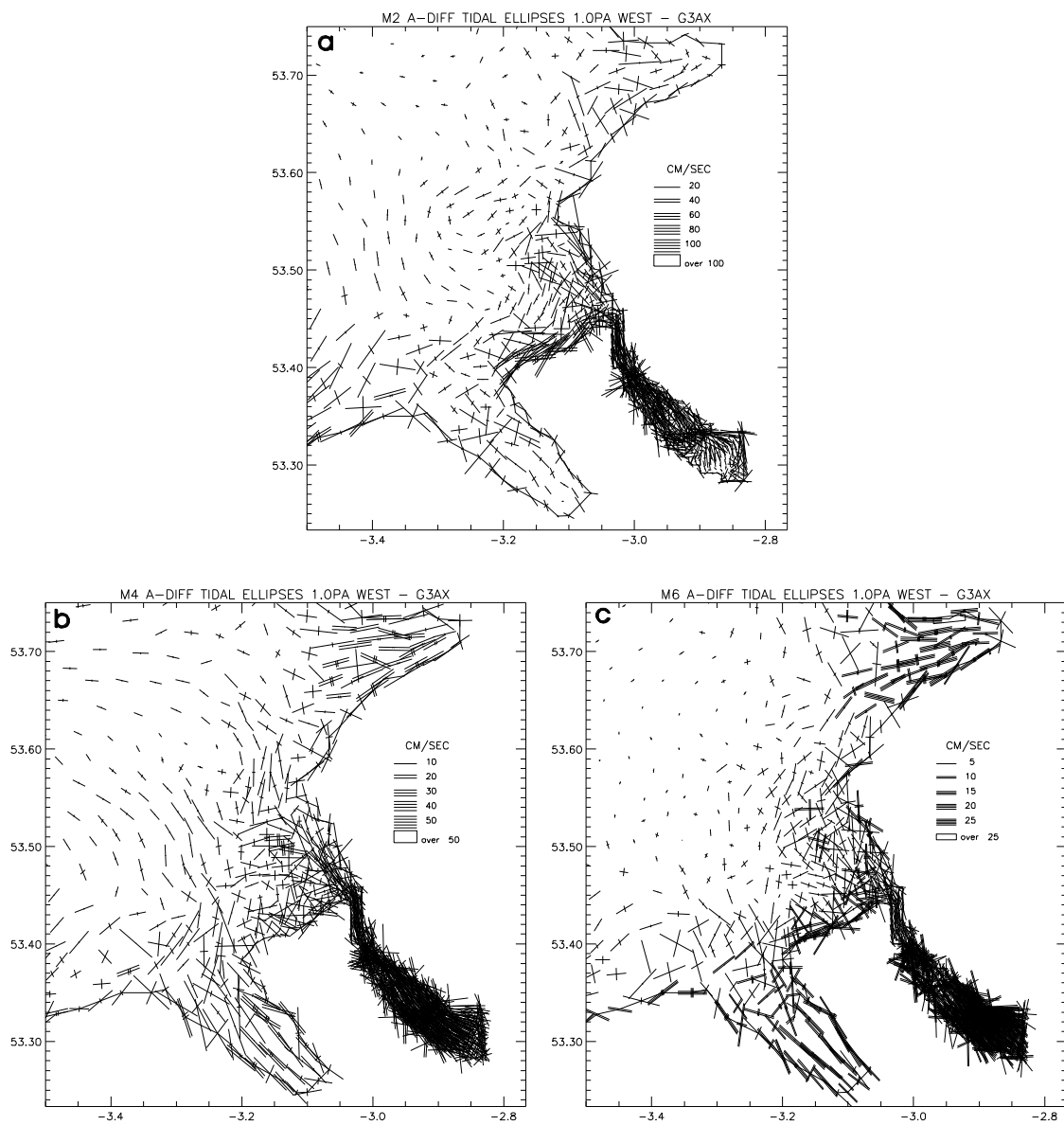
1 FIG 17



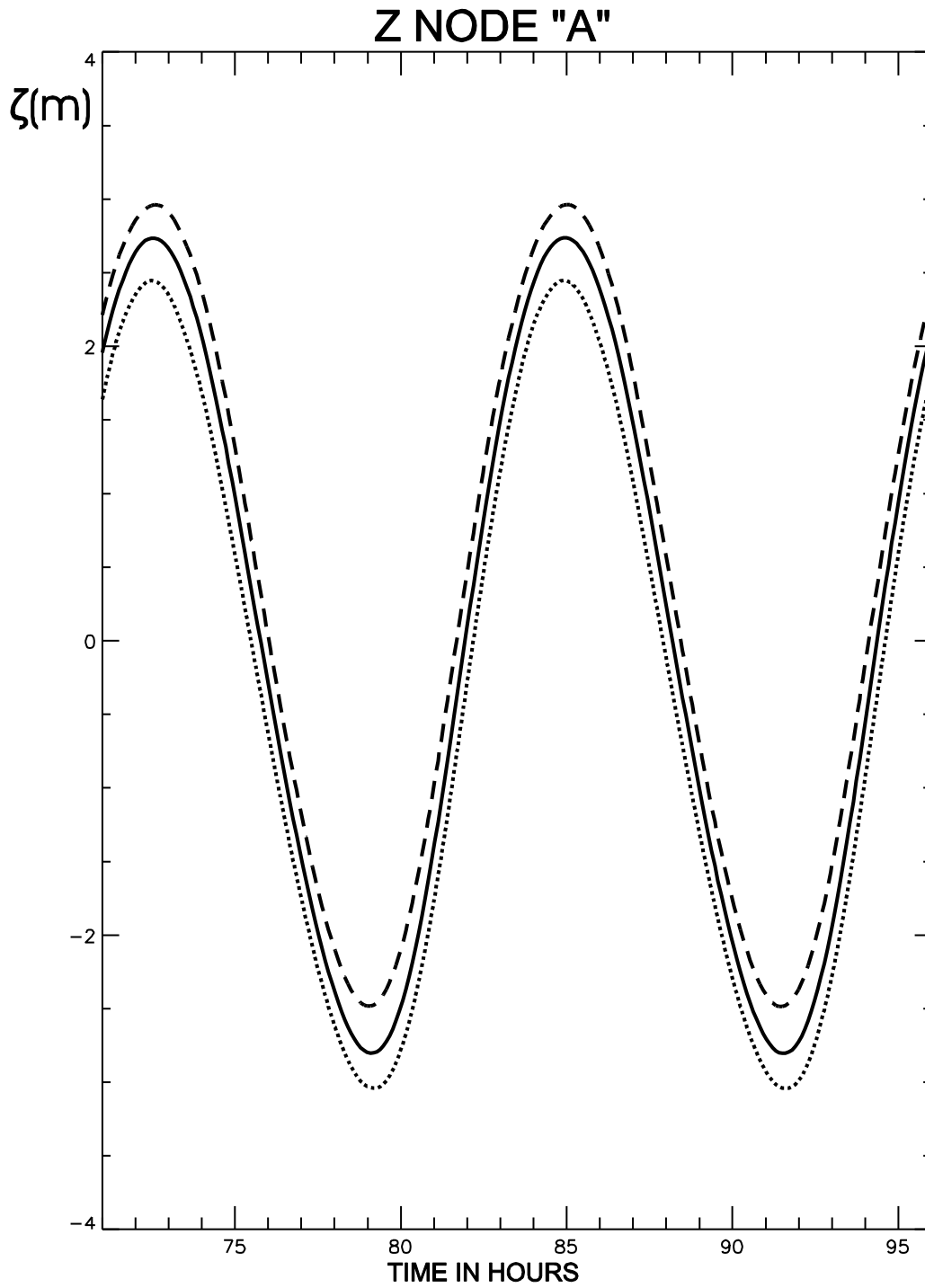
2
3
4



1 FIG 19

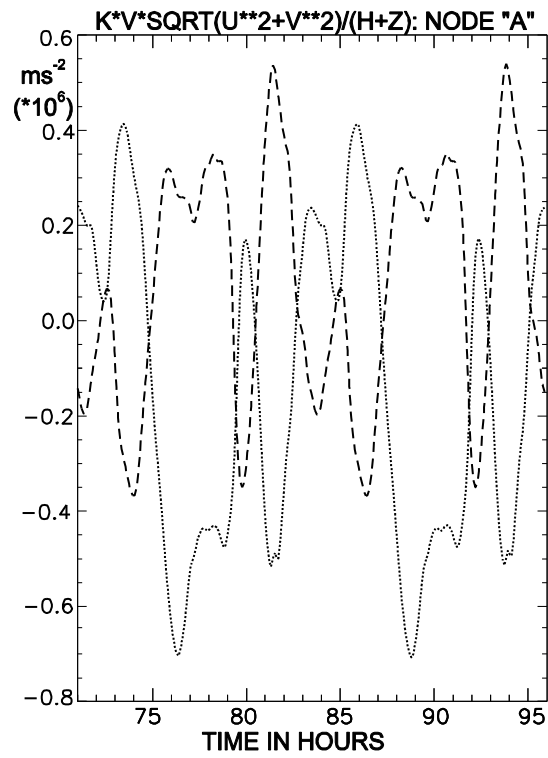
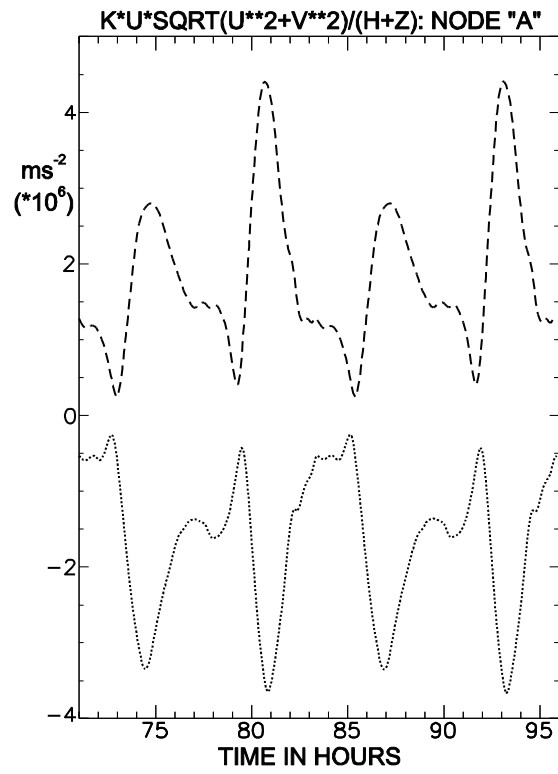


2
3
4



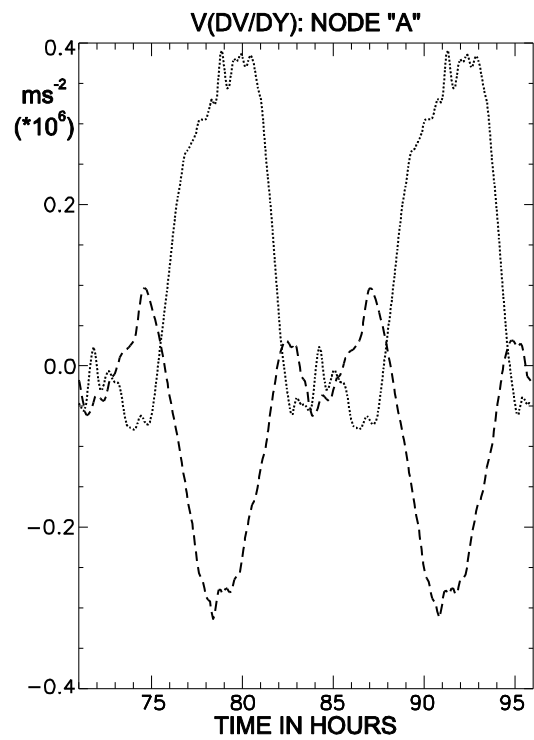
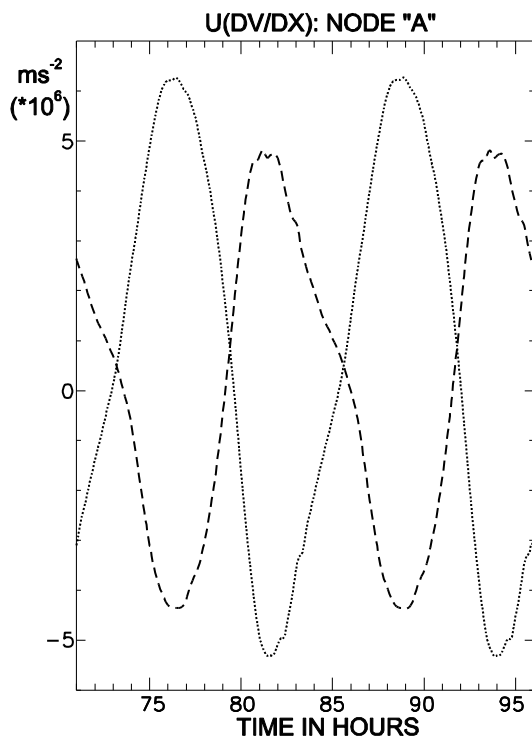
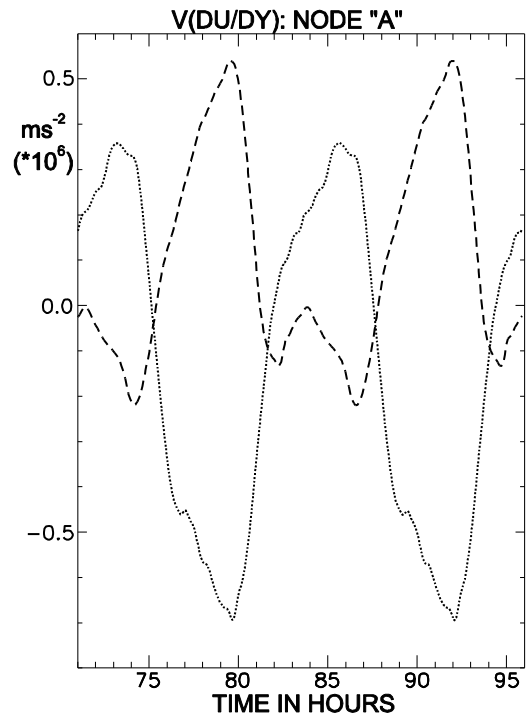
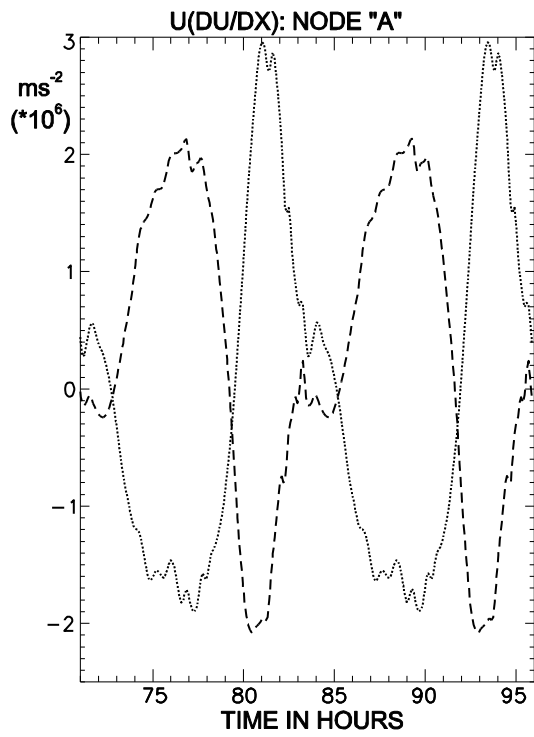
2
3
4

1 FIG 21

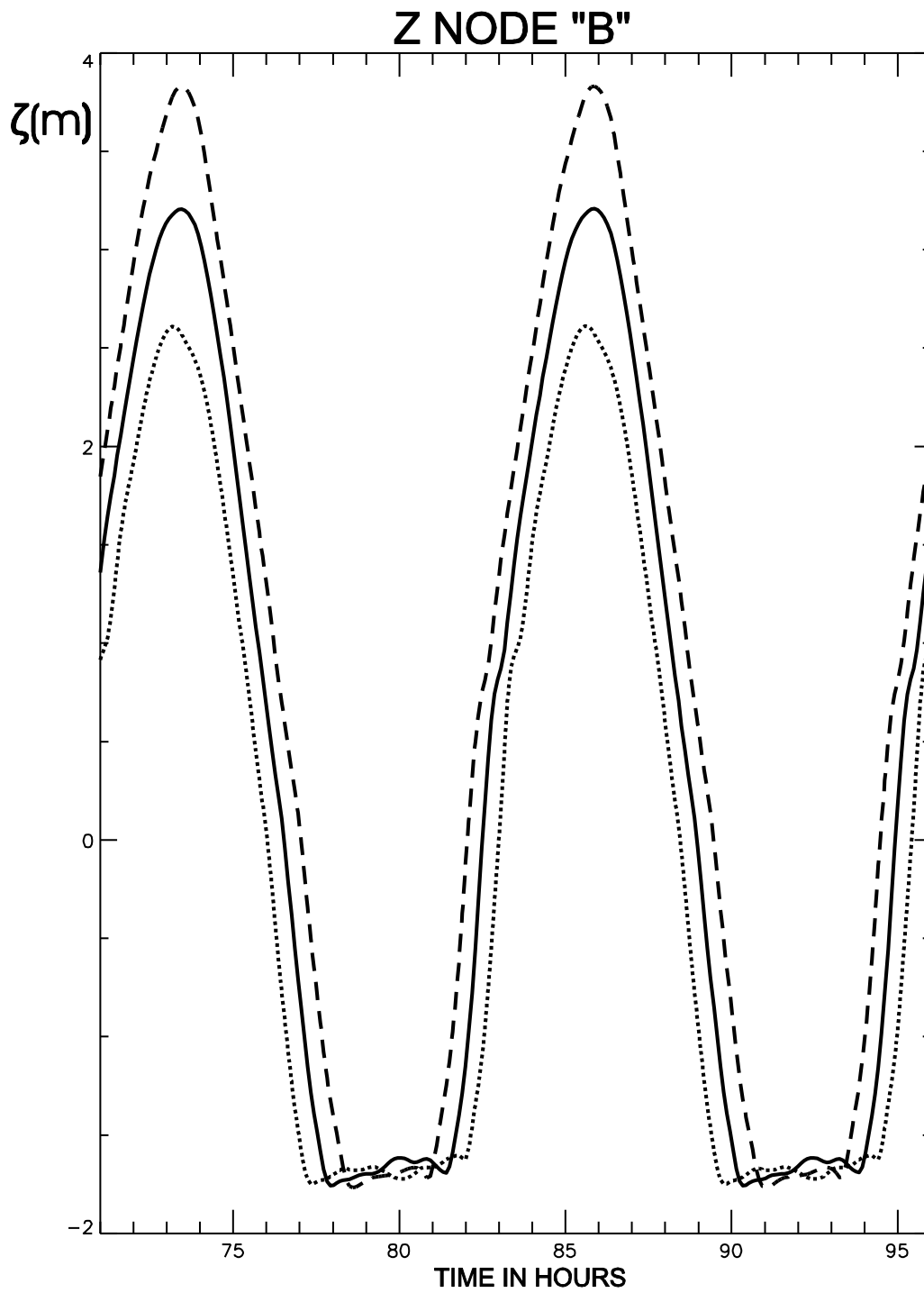


2
3
4

1 FIG 22

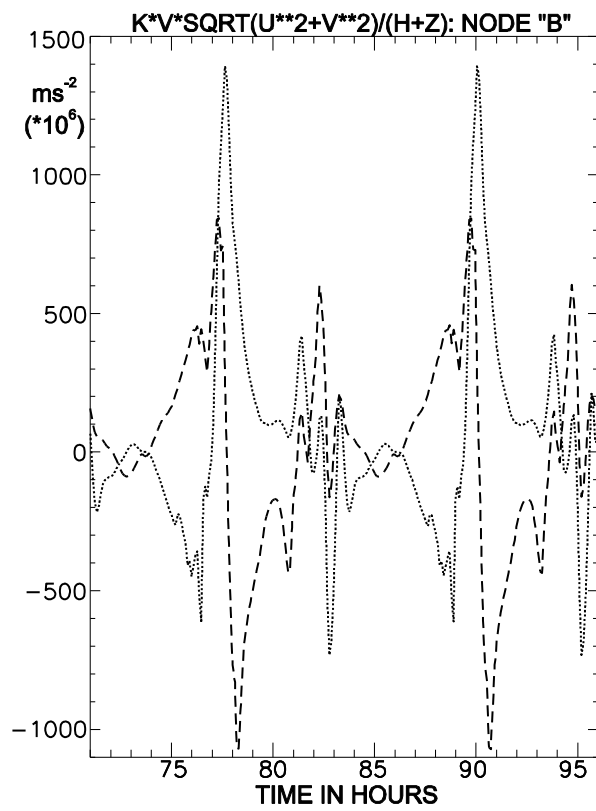
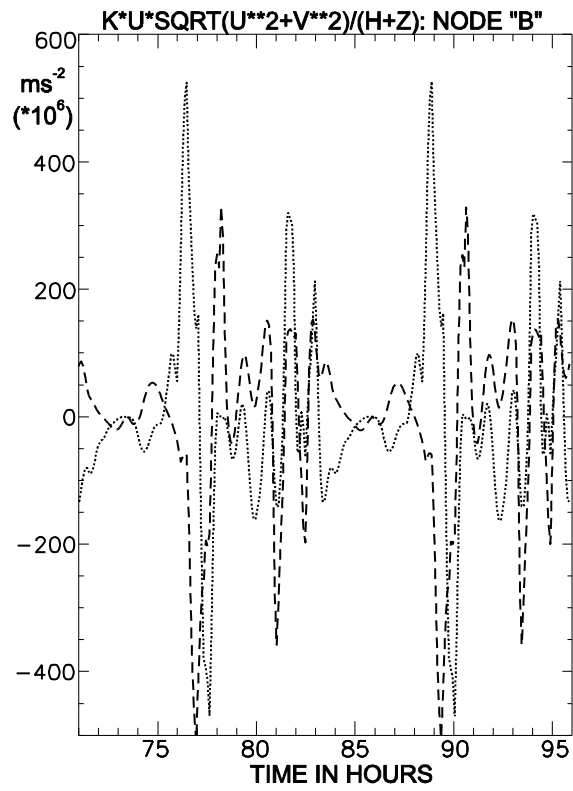


2
3
4



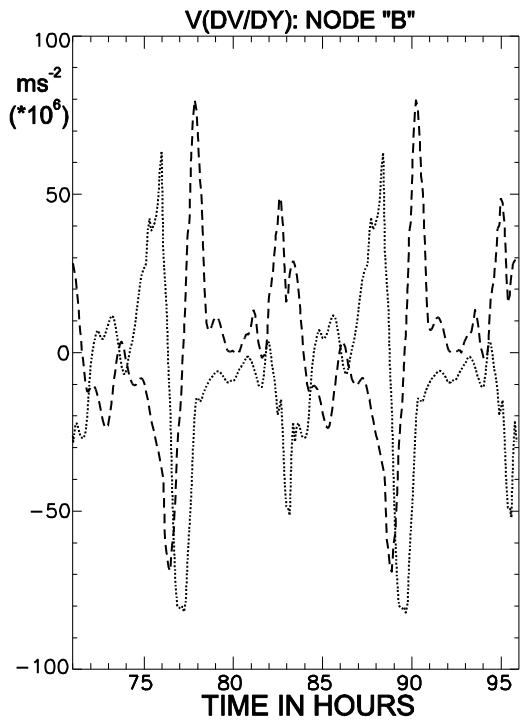
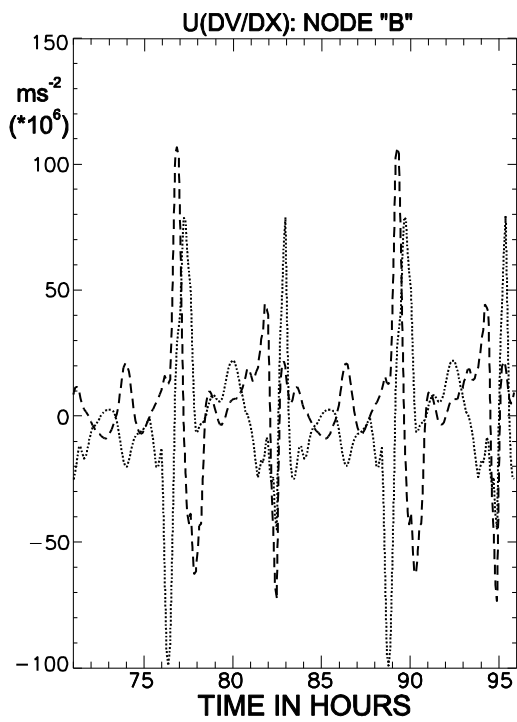
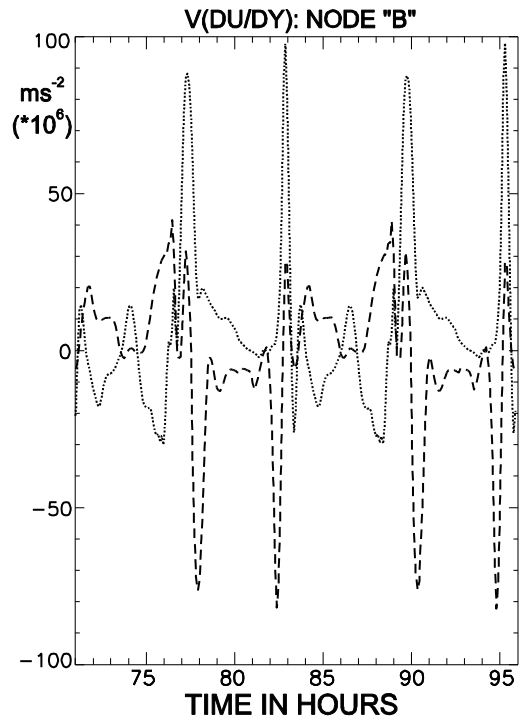
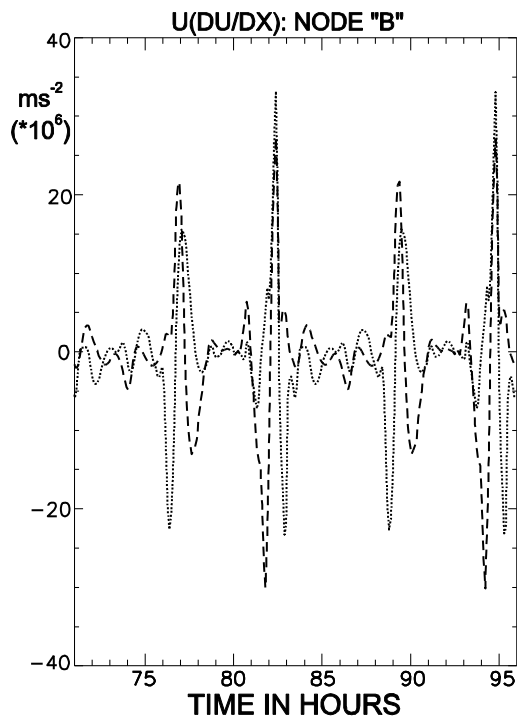
2
3
4

1 FIG 24



2
3
4

1 FIG 25



2
3
4